Research Square

Preprints are preliminary reports that have not undergone peer review.
They should not be considered conclusive, used to inform clinical practice,
or referenced by the media as validated information.

A novel digestive symbiont for both holobiont Rimicaris exoculata and Rimicaris chacei: the case of Lachnospirales

Marion Guéganton
Univ Brest
Léna Ailliot
Univ Brest
Johanne Aubé
Univ Brest
Valérie Cueff-Gauchard
Univ Brest
Lucile Durand
Univ Brest
Marie-Anne Cambon
marie.anne.cambon@ifremer.fr
Univ Brest

Research Article

Keywords: Rimicaris spp, Holobiont, Digestive symbiosis, Metagenomics, Lachnospirales, Fluorescent in situ Hybridization, Metabarcoding, Acquisition, Hydrothermal vent, Immunity

Posted Date: March 8th, 2026

DOI: https://doi.org/10.21203/rs.3.rs-7823722/v1

License: This work is licensed under a Creative Commons Attribution 4.0 International License. Read Full License

Additional Declarations: No competing interests reported.

Abstract

Background

In deep-sea hydrothermal vents ecosystems, most animals harbor symbiotic communities supporting their nutrition. This is the case of both shrimps *Rimicaris exoculata* and *Rimicaris chacei*, two endemic species of the Mid-Atlantic Ridge (MAR), housing three distinct bacterial symbiotic communities playing a major role in their nutrition and scaling up their immune systems. One is located in the cephalothoracic cavity, the second in the foregut and the last one in the midgut, mostly represented by *Candidatus* Microvillispirillaceae. However, recent metabarcoding and metagenomics studies reported for the first time the presence of another abundant potential digestive symbiont representing a novel family of *Lachnospirales*. To date, their role and structuration in the holobiont remain unknown. We combined Fluorescent *in situ* Hybridization, metabarcoding and genome-resolved metagenomics data to reveal a part of their evolution, contribution to the holobiont functioning and their metabolic potential. For this, we used the raw reads of a recent metabarcoding analysis and Metagenome-Assembled Genomes (MAGs) obtained in a previous study.

Results

We studied two MAGs reconstructed from TAG and Snake Pit sites (MAR) revealing a novel digestive *Lachnospirales* family in the midgut. This novel symbiont showed the capacity to degrade host's chitin, to fix carbon dioxide thanks to secondary pathways, to use oxygen and to encode for flagellar genes implied in host-symbiont recognition. In addition, they harbor CRISPR/cas genes that may be involved in the holobiont defense. *Lachnospirales* seemed to colonize the ectoperitrophic space, were submitted to elongation without dividing themselves and are acquired post-installation of the juveniles on active sites. Consequently, they share many commonalities with *Candidatus* Microvillispirillaceae, which they co-occur with.

Conclusion

Our data suggest that the *Lachnospirales* would be mixotrophic and would live in syntrophy with *Candidatus* Microvillispirillaceae. Indeed, they could degrade chitin, allowing *Ca.* Microvillispirillaceae to use degradation products for their metabolism. As *Ca.* Microvillispirillaceae, they are acquired post-installation during metamorphosis. Consequently, both symbionts may strongly contribute to the holobiont fitness.

Background

In deep-sea hydrothermal vents, life is sustained by microbial primary production [1], metazoans relying on chemosynthetic microorganisms for their nutrition. In many cases, microbial communities are symbiotic, living in intimate associations with metazoans. Host with its associated symbionts is called holobiont [2]. Holobionts dominate these extreme ecosystems [1, 3] and are considered as a single entity according to their long-term association, involving the emergence of new structures and metabolisms [2, 4–6]. In deep-sea hydrothermal vents, species such as *Riftia* tubeworms, *Bathymodiolus* mussels or *Alviniconcha* gastropods [7–9] have developed symbiotic relationships in specialized organs or cells. This is also the case for two alvinocaridid shrimp species co-occurring at the active vents of the Mid-Atlantic ridge. *Rimicaris exoculata* and *Rimicaris chacei* [10] harbor both three diversified symbiotic bacterial communities they rely on [11].

A first symbiotic community is established in their cephalothorax playing a major trophic role for *R. exoculata* (trans-cuticular absorption of nutrients) [12–14], contrary to *R. chacei*, showing a mixotrophic diet based on symbiotic relationship, bacteriotrophy, predation and scratching [15, 16]. Even if this symbiotic relationship provides most nutrients (up to 80% of carbon source for *R. exoculata* [17]), two other distinct bacterial communities colonize the digestive system [16, 18–21] composed of the foregut (esophagus and stomach), the midgut (hepatopancreas and midgut tube) and the hindgut. Although the digestive system of *Rimicaris* spp. is usually full of minerals and can contain cuticle particles, it is functional with an active alimentary bolus transit [19]. After 72 hours of starvation or after molting, symbiotic bacteria are still present [20] reinforcing the hypothesis of their implication in immunity, nutrition and nutrients absorption [19].

The foregut digestive symbiotic community is mainly composed of *Candidatus* Foregutplasma rimicarensis and *Candidatus* BG2_rimicarensis [19]. These symbionts are attached to the setae of the pyloric chamber (stomach) and esophagus [18] and submitted to molt (ectodermic origin). They seem to be involved in the host defense and could metabolize intermediate products of chitin degradation [18]. The midgut symbiotic community is mostly composed of *Candidatus* Microvillispirillaceae [18, 19]. Like *Ca.* Foregutplasma rimicarensis and *Ca.* BG2_rimicarensis. These symbionts seem to be involved in host's immunity, in complex polymers degradations and vitamins synthetization. Moreover, they have numerous genes involved in motility and chemotaxis [19]. A surprising fact about *Ca.* Microvillispirillaceae is their location and morphology within the midgut tube. They are long and thin bacterial cells inserted between microvilli of the intestinal epithelium in the ectoperitrophic space [18, 20, 21]. For decapods, this space is protected and separated from the alimentary bolus by the peritrophic membrane, keeping this zone sterile [22]. This could strengthen the hypothesis of the defensive role of these symbionts for the holobiont. Another intriguing point is that they exhibit no cell division while having the genes encoding chromosome replication and cell division, suggesting they would be under host control [16, 18–21]. Moreover, *Ca.* Microvillispirillaceae are heterotrophic symbionts relying on their host or other symbiotic bacteria [19]. According to recent studies, a potential candidate for bacterial syntrophy could be *Lachnospirales* (*Clostridia* class). Indeed, two MAGs (Metagenome-Assembled Genomes) affiliated to *Clostridia* have been identified in a previous metagenomic analysis of the digestive system of *R. exoculata* with a higher abundance in the midgut tube (Aubé et al., 2022 [19]). However, this bacterial class is usually considered as ubiquist, so full identification and analysis were not undertaken. In 2024, a metabarcoding analysis was published in Guéganton et al., 2024 [23] study. These *Clostridia* were retrieved at different life stages and have been affiliated to *Lachnospirales*. They were limited to the midgut tube samples, suggesting a possible symbiotic relationship between this lineage, *Ca.* Microvillispirillaceae and the host. Another study dealing with host sex, habitat and vent fields potential effect on microbial diversity (free-living and symbiotic communities), showed that *Lachnospirales* were only recovered in the midgut tube, reinforcing the hypothesis of a symbiotic relationship at juvenile stages [23], and adult stages. The presence of *Lachnospirales* in the midgut tube of both *R. exoculata* and *R. chacei* specimens has been demonstrated, but they still have never been observed and their functions for the *Rimicaris* holobiont are still unknown.

Lachnospirales (Bacteria, phylum *Bacillota-A*, class *Clostridia* – according to GTDB) may play a major role in holobiont fitness both in terms of nutrition and immunity. This order is retrieved in many hosts, both terrestrial and aquatic. *Lachnospiraceae* (*Lachnospirales* order – according to GTDB) takes part of the intestinal microbiota of mammals like zokors, mice, chinchillas and humans [24–27]. For these host species, *Lachnospirales* are a major actor of the holobiont fitness. They can degrade complex carbohydrates like cellulose and other sugars, producing fatty acids necessary for intestinal epithelium cell nutrition [24]. Some *Lachnospirales* (*Lachnospiraceae*_NK4A136_group genus) are fiber-degrading bacteria leading to the production of butyrate, a fatty acid playing as an intestinal barrier (decrease of inflammation, anti-tumor effects) [27]. They can also help fighting obesity [25]. However, although most *Lachnospirales* are candidates for holobiont immunity, according to their abundance and the taxa represented, they can lead to intra- and extra intestinal diseases [27]. *Lachnospirales* are also part of the digestive microbiome of mesopelagic animals. For example, for *Cyclothone* species and *Vampyroteuthis infernalis*, the *Lachnospiraceae* family is significantly represented among their digestive bacterial communities [28]. The omnipresence of *Lachnospirales* in different host digestive systems would highlight the importance of such symbionts along evolution and particularly here in *Rimicaris* spp.

Regarding *R. chacei* and *R. exoculata* species, recent studies focused on juvenile stages [14, 23]. *R. chacei* juveniles live in nurseries separated from the adults whereas *R. exoculata* juveniles gather in patches near adult *R. exoculata* aggregates [29, 30]. Juveniles are recognizable from adults due to their red/orange lipid storage color [14, 31] and an entire revision of their taxonomy has been established avoiding potential misidentifications at early stages [14]. On sites, three juvenile stages have been identified for *R. exoculata* (A, B and subadult) against two for *R. chacei* (A and subadult) [14]. Combining taxonomic identification, *i.e COI – cytochrome oxidase I* – sequencing and 16S rRNA metabarcoding approaches on *R. exoculata* and *R. chacei* juvenile specimens from TAG and Snake Pit, a first comprehensive dataset of symbiotic communities colonizing each symbiotic organ has been provided [23]. This study shed light on hypotheses regarding the transmission and acquisition of major symbionts in the digestive system. To ensure the maintenance of symbiotic relationships, symbionts can be transmitted either horizontally – from the environment – or vertically – from the parents [7, 8, 32, 33]. Furthermore, this study proposed that *Ca.* Foregutplasma rimicarensis, *Candidatus* BG2_rimicarensis and *Ca.* Microvillispirillaceae would be acquired post-settlement

on site suggesting a mixed transmission (release of symbionts from adults in the environment before juvenile colonization) [23]. With the recent discovery of *Lachnospirales* midgut colonization, the question of their acquisition and transmission is entirely open. Because they co-occur in the midgut tube with *Ca.* Microvillispirillaceae, it seems essential to understand the relationship between both and understand their potential co-evolution within the holobiont.

To study the potential function and acquisition of the *Lachnospirales* in the digestive system of both *R. exoculata* and *R. chacei* species, we combined three molecular approaches: Fluorescent *in situ* Hybridization, metagenomic and metabarcoding, using MAGs and raw data from two previous studies [19, 23]. We focused on specimens from two hydrothermal vents, TAG and Snake Pit (MAR), presenting contrasted geochemical environments [34]. First, we focused on the identification of the symbionts using Fluorescent *in situ* Hybridization (FISH) microscopy. We developed and optimized a new specific probe to both combine symbiotic cell visualization and identification along the midgut tubes. Then, functional analyses of MAGs allowed us to investigate the potential role of a novel family of *Lachnospirales* from *R. exoculata* adult specimens, while metabarcoding allowed us to gain insights into the questions of acquisition, transmission and installation of the symbiont for both species at each life stage. To perform metabarcoding analysis, we used raw reads from Guéganton et al., 2024 [23] combined with new ones obtained from adults. For metagenomics analysis, we annotated and investigated two *Lachnospirales* MAGs obtained in Aubé et al., 2022 [19]. The combination of FISH, metagenomic and metabarcoding approaches was used to answer the following questions: 1) What is the distribution and abundance of *Lachnospirales* in the digestive system of both *Rimicaris* species from stage A to adult stages? 2) What is the dynamic of the symbiont colonization throughout juvenile development? 3) What are the potential roles of the symbiont in the holobiont fitness? We present the results of these investigations, discuss the potential role of *Lachnospirales* in the holobiont and suggest a syntrophy between co-occurring symbionts.

Methods

Sample Collections

Samples were collected at two vent fields along the Mid-Atlantic Ridge (MAR): TAG (26°08' N—44°49' W, 3660 m depth) and Snake Pit (23°23' N—44°58' W, 3480 m depth) during the BICOSE2014 cruise (January 2014, https://doi.org/10.17600/14000100) for metagenomic and metabarcoding analyses, the BICOSE2 cruise (February 2018 https://doi.org/10.17600/18000 004) for fluorescent microscopy and metabarcoding and the HERMINE cruise (16 March to 27 April 2017, https://doi.org/10.17600/17000200) for metabarcoding analyses (**Supplementary Table 1**). Specimens were collected in shrimp aggregations or nurseries (depending on the stage) using the suction sampler of the ROV Victor 6000 (Remotely operated Vehicle), or the HOV Nautile (Human Occupied Vehicle), operated from the Research Vessel "*Pourquoi pas*?". For FISH studies, some shrimps were immediately dissected under sterile conditions and tissues were fixed in a 3% formalin seawater solution for 3 hours to keep cell integrity. Then, they were rinsed with a phosphate-buffered saline solution (PBS) and stored in a PBS/ethanol (1:1) solution at -20°C [19]. Adult shrimp for metabarcoding study were dissected under sterile conditions, quickly passed through liquid nitrogen and dry-conditioned at -80°C. Other specimens were fixed frozen at -80°C for later dissections at the laboratory for DNA extraction (juvenile samples for metabarcoding and adult samples for metagenomics) or fixation for FISH. The detail of specimens treated for metabarcoding (juveniles), and metagenomic analyses can be retrieved respectively in Guéganton et al., 2024 [23] (**Supplementary Material 1**) and Aubé et al., 2022 [19] (**Supplementary Material 4**).

DNA extraction, amplification and sequencing

In this study, we focused on midgut tube samples. For juvenile midgut tube samples (**Supplementary Table 1, Supplementary Material 1)**, we reanalyzed the raw reads obtained in Guéganton et al., 2024 [23]. For complete details on DNA extraction from muscle for COI sequencing (Omega BIO-TEK E.Z.N.A Tissue DNA® kit) and from symbionts (Macherey-Nagel NucleoSpin Soil® kit), amplification (primers Cari-COI-1F/Cari-COI-1R for COI, Whoi341/Whoi785 and E8F/907R for bacterial 16S rRNA gene) sequencing (Sanger Sequencing for COI and Illumina Miseq for bacterial 16S rRNA gene) please refer to the Materials and Methods from Guéganton et al., 2024 [23] (**Supplementary Material 1)**. To complete our study, we used midgut tube samples of *Rimicaris exoculata* adult specimens from TAG and Snake Pit (BICOSE2 cruise, **Supplementary Table 1**), some of which were

collected from dense aggregations and others were scattered individuals. Specimens were aseptically dissected, and midgut tube samples were extracted with the Macherey-Nagel NucleoSpin® Soil Kit following the manufacturer instruction and using SL2 buffer for the chemical lysis. To ensure the mechanical lysis, we used the Bead-Beater FastPrep® 1120 (MP Biomedicals) for 30s with an intensity of 5.5 m/sec. To finish, elution was carried out with 60 µL of pre-warmed SE buffer. As for juvenile samples, direct amplification of the bacterial 16S rRNA gene was performed using universal primers Whoi341 and Whoi785 [35] with adaptors. Direct amplifications were performed as described in **Supplementary Material 2**. Then the PCR products were purified using Macherey-Nagel NucleoSpin® and PCR clean-up kit before they were carried out using the Genotoul GeT PlaGe platform (INRAE, Castanet-Tolosan, France) as for juvenile samples. Samples were sequenced using an Illumina MiSeq platform with a paired-end read length of 2×250 bp with chemistry V3. To complete and confirm the data analyses, we also used midgut tube samples of *Rimicaris exoculata* and *Rimicaris chacei* adult specimens from TAG and Snake Pit obtained during BICOSE2014 cruise (**Supplementary Material 3)**.

For the metagenomic analyses, the two MAGs we focused on were obtained from specimens analyzed in Aubé et al., 2022 [19] (**Supplementary Material 4)**.

Metagenomics Analyses

We analyzed two MAGs (M_TAG_MAG_00001 and M_SnakePit_MAG_00001) obtained in a recent study by Aubé et al., 2022 [19], affiliated to *Clostridia* but never further analyzed. The entire process to reconstruct the MAGs that were analyzed are described in the Metagenomic analysis of the Methods part of Aubé et al., 2022 [19] (**Supplementary Material 4)**. In this study, we first reassessed the MAGs completeness and redundancy using CheckM2 v1.0.1 [36]. The Average Nucleotide Identity (ANI) between both MAGs was calculated with FastANI. v1.3 [37]. Then, to build the phylogenomic tree, the 120 marker genes were identified in the MAGs with the gtdb-tk v2.4.0 [38] “identify” command and aligned to the marker genes of all representative *Lachnospirales* genomes from GTDB with the “align” command. The position presenting gaps in at least 50% of the sequences in the resulting Multiple Sequence Alignment were trimmed using TrimAl v1.4.1 [39]. *Lutisporales* were used as an outgroup. The Maximum Likelihood tree was finally reconstructed with IQ-Tree v2.0.3 [40] (1000 bootstrap, WAG model). It was then visualized with ggtreeExtra package from RStudio. Annotation of the MAGs was done with Prokka v1.14.6 [41] and the KEGG-Kofam before using KEGG module completeness was investigated using the “anvi-estimate-metabolism” program from Anvi’o v8 [42]. We also used the EGGNog annotation results from the MicroScope Microbial Genome Annotation and Analysis Platform (MaGe; https://mage.genoscope.cns.fr/) [43]. The carbohydrate-active enzyme (CAZyme) encoding genes were identified using dbCAN3 v3.0.4 [44]. Finally, genes involved in the CRISPR-Cas system were found using CRISPRCasFinder online version. Only hits showing at least an evidence level of 4 were considered. Schematic representations of the predicted metabolic potential pathways were constructed using Inkscape.

Metabarcoding Analyses

In this study, a 16S DNA metabarcoding analysis was performed first using both raw data from juvenile midgut tube specimens obtained in Guéganton et al., 2024 [23] and adult midgut tube specimens obtained during the BICOSE2 cruise (**Supplementary Material 5)**. To confirm and complete the results, a second analysis was performed on *R. exoculata* and *R. chacei* adult midgut tube specimens from TAG and Snake Pit obtained during the BICOSE2014 cruise independently (**Supplementary Material 6)**.

Metabarcoding data analysis was processed using SAMBA v4 (Standardized and Automated Metabarcoding Analyses, https://gitlab.ifremer.fr/bioinfo/workflows/samba), an open-source workflow developed at Ifremer (SEBIMER). It uses a NextFlow workflow manager [45] that automates and standardizes the analysis of metabarcoding data through a suite of “standard” sequence treatment software. SAMBA is based on the QIIME 2 v2022.11 pipeline [46] and first consists of checking the raw data integrity and metadata. Then these data are formatted to create a QIIME 2 object. Data are cleaned and filtered to remove sequencing primers and barcodes from adapter using Cutadapt v.4.2 [47]. Then, the FIGARO tool [48] was used to optimize quality filters and minimize errors during ASV clustering using DADA2 v.1.26 [49]. Then the dbOTU3 v.1.5.3 algorithm [50] was executed to refine clustering ASV (sequence similarity and abundance profile) to consider the overestimation of diversity produced by DADA2. MicroDecon v.1.0.2 [51] was also used to decontaminate samples by comparing them to sequenced negative controls for the first analysis (extractions, PCR and purification blank) (**Supplementary Material 5)**. The

taxonomic assignment was achieved using the SILVA 138.2 reference database [52] and 16S_V3-V4_341F-785R or 16S_V3-V5_357F-926R (receptively **Supplementary Material 5 and 6)**. subcollection was used for bacteria. An additional and optional tool ANCOM-BC (ANalysis of COmposition of Microbiomes with Bias Correction) [53] was used to perform microbiome composition analysis.

The final step of SAMBA consists in statistical analysis of α-diversity and β-diversity. We used Chao1 index (estimate the expected richness) and Shannon index (number of ASVs, abundance and distribution) to estimate the species richness and diversity within each sample based on ASVs dataset (α-diversity). ANOVA (Analysis of the Variance) tests were performed to compare the α-diversity between species, sites and stages with both indexes. SAMBA also takes into account the interspecific diversity of communities (β-diversity). In this study, diversity analyses were achieved by ordination method using Principal Coordinates Analysis (PCoA) based on Unifrac (presence/absence of ASVs) and Weighted Unifrac (W-Unifrac – abundance of ASVs) – both based on taxonomic proximity of the ASVs detected – calculated on a normalized ASVs dataset DESeq2 [54]. The script includes a multivariate analysis of variance by permutations (PerMANOVA) using the Adonis2 function of the Vegan package to assess the influence of site, species and life stage on bacterial community. The R © software v. 4.4.2 (R Core Team, 2024) was used to perform statistical analyses and produce data visualizations. For better graphic representation, we focused on barplot showing the main lineages retrieved in the midgut tube at the Order level.

In silico design and validation of a new FISH specific probe Clostri-Lachno109

We developed a new probe specially targeting the *Lachnospirales* symbiont lineage. We used 16S rDNA sequences obtained by PCR cloning approaches [16, 20, 21] and metabarcoding analysis from Guéganton et al., 2024 [23] to design *in silico* the probe. Then we used the MUSCLE (MUltiple Sequence Comparison by Log- Expectation) algorithm [55] in Geneious software v9 [56], literature data [57, 58], Geneious Primer Design tool and the Oligo Calc [59] and BLAST [60] with the Silva138 database (test probes v3.0) to validate the probe as described in the Material and Methods of Guéganton et al., 2022 [18].

Fluorescent *in situ* Hybridization and optimal hybridization conditions for the new Clostri-Lachno109 probe

To ensure the specificity of the probe Clostri-Lachno109, the samples were prepared according to the protocol from Guéganton et al., 2022 [18]. Samples were dehydrated in PBS/ethanol series at temperature room, then immersed into ethanol/resin at 40°C (Polyethylene glycoldistearate-1-hexadecanol (9:1), Sigma-Aldrich, Merck KGaA, Darmstadt, Germany), before being embedded into the PEG resin. Resin blocks were stocked at -20°C after polymerization and were trimmed into 8 µm transversal tissues sections with a RM 2255 microtome (Leica Biosystems, Nussloch, germany) and placed on slides (Menzel-Gläser Superfrost Plus, USA). Resin was removed with three ethanol baths (96%) before the tissues were partially rehydrated in an ethanol bath (70%). Optimal probe hybridization conditions were determined using host tissues known to lack (e.g. cephalothorax mouthparts, foregut) or harbor (e.g. midgut tube) these target symbiont lineages. GAM42a [61] and Epsy549 [62] targeting respectively *Gammaproteobacteria* and *Campylobacteria*, Def1229 targeting *Ca.* Microvillispirillaceae and Myco1-378 targeting *Hepatoplasmataceae* [18] were used respectively as positive controls on cephalothorax mouthparts, on midgut tube and foregut. The universal probe Eub338-I targeting most Eubacteria [63] was used as a general positive co-hybridization control (Table 1). All probes were synthesized by Eurofins Genomics (Ebersberg, Germany) and were labelled with either ATTO488, Cyanine 3 or Cyanine 5 dyes (Table 1).

Table 1
Probes used for this study.

Target	Probe	Sequence (5'-3')	Dye	Location (rRNA gene)	Optimal Formamide %	References
Bacteria	**Eub338**	**GCTGCCTCCCGTAGGAGT**	**ATTO488**	**338 (16S)**	**30**	**[63]**
Candidatus Microvillispirillaceae	**Def1229**	**GCCCTCTGTATAGTCCATTG**	**cy5**	**1229 (16S)**	**30**	**[17]**
Hepatoplasmataceae	Myco378-1	GTGGAAAATTCCCTACTGCTG	cy5	378 (16S)	45	[17]
Lachnopsirales	Clostri-Lachno109	GGCAGGTTACTCACGCGTTA	cy3	109 (16S)	30	This study
Gammaproteo-bacteria	GAM42a	GCCTTCCCACATCGTTT	cy5	1027 (23S)	30	[61]
Campylobacteria	Epsy549	CAGTGATTCCGAGTAACG	ATTO488	549 (16S)	30	[62]

Optimal stringency conditions were determined using different combinations of formamide concentrations in the hybridization buffer and both hybridization and washing temperatures. Sections were labeled in reaction mix containing probes (each at 0.5µM final concentration) in a hybridization buffer [0.9M NaCl, 0.02M Tris-HCl [pH 7.5], 0.01% [w/v] sodium dodecyl sulphate (SDS), 20%, 30%, 45% deionized formamide], incubated for 3 hours at 46°C or 48°C (Table 2). After hybridization, sections were briefly pre-rinsed and were then washed for 15 min in a rotary oven at 48°C or 50°C (Table 2), in a washing buffer [0.215M, 0.102M, 0.03M NaCl respectively for 20%, 30%, 45% formamide, 0.02M Tris-HCl [pH 7.5], 0.005M EDTA [pH 8] and 0.01% [w/v] SDS]. Sections were then briefly rinsed with distilled water, first at washing temperature (48°C or 50°C), then at room temperature. Sections were mounted on slides with SlowFade™ Gold antifade reagent with DAPI (Invitrogen). Observations on hybridized tissues were made using a Zeiss Imager.Z2 microscope equipped with the Apotome.2® sliding module and Colibri.7 light technology (Zeiss, Oberkochen, Germany). The micrographs were analyzed using the Zen software (Zeiss). Differential Interference contrast (DIC) was used to better visualize the host tissues and bacteria.

Table 2
Hybridization and washing conditions tested.

Conditions/Samples	Subadult Cephalothorax Mouthparts	Adult Midgut tube	Adult Foregut
Formamide (hybridization buffer)	**30%**	**20% – 30%**	**30% – 45%**
Hybridization temperature	**46°C**	**46°C and 48°C**	**46°C**
Washing temperature	48°C	48°C and 50°C	48°C

Chromosomes visualization

To visualize bacterial chromosomes in *Lachnospirales* cells, we used a highly DNA-specific dye: YOYO™-1dye (Invitrogen). Slides from hybridized sections were removed and the sections were rinsed abundantly with water at room temperature. Once dry, the sections were labeled in a 30µl aqueous solution containing 10-2mM YOYO™-1 dye for 15 min at room temperature and then washed with water. Then sections were mounted on slides with Citifluor AF1 antifade solution (Electron Microscopy Sciences, Hatfield, PA, USA). We performed observations using a LSM 780 confocal microscope (Zeiss) to reveal the fluorescence and analyze/quantify it as a spectrum. Micrographs were done with Zen software (Zeiss).

Code and data availability

The metagenomes raw reads used for this study are available in the European Nucleotide Archive under Bioproject Accession Number PRJEB50056 Aubé et al., 2022 [19], The URL https://gitlab.ifremer.fr/rimicaris/rimicaris-exoculata-gut-epibionts-metagenomes provides access to a detailed reproducible bioinformatics workflow for the reconstruction of the MAGs. FASTA

files for individual metagenomic assemblies, FASTA files for the MAGs, and Anvi'o merged profile databases of the dereplicated MAGs are available with this URL https://doi.org/10.12770/437f34c4-aba3-4962-9f6f-4c469defc483. The analyses performed for the metabolic investigations of this paper are described here: https://gitlab.ifremer.fr/rimicaris/novel-digestive-symbiont-lineage-of-lachnospirales-within-2-rimicaris-species

The raw reads of the metabarcoding dataset are available in the European Nucleotide Archive under Bioproject Accession Number PRJEB71821 (https://www.ebi.ac.uk/ena/browser/view/PRJEB71821) Guéganton et al., 2024 [22], PRJEB97771 (https://www.ebi.ac.uk/ena/browser/view/PRJEB97771) and PRJEB97765 (https://www.ebi.ac.uk/ena/browser/view/PRJEB97765). The configuration files for the process's options used in SAMBA are available in the **Supplementary Material 4**. The COI sequences of juveniles are available on NCBI under accession numbers PP916018-PP916042 (**Supplementary Table 1)**.

Results

Symbiotic communities of the midgut tube

The metabarcoding analyses were conducted to compare the presence or absence and the relative abundance of digestive symbionts according to the life stage, the site and the species (**Supplementary Table 2**). The main analysis on juvenile and adult specimens showed no significant variation in bacterial richness and abundance with life stages, species or site (**Supplementary Fig. 1)**. However, β-diversity with PCoA plots showed a difference between vent sites (**Supplementary Fig. 2A, B**) for both Unifrac and W-Unifrac distances, whereas PCoA plots for life stages are less marked and overlapped largely within each species for W-Unifrac and Unifrac distances (**Supplementary Fig. 2D-F**). The same tendency was confirmed by the results of the second metabarcoding analysis on *R. exoculata* and *R. chacei* adult specimens from BICOSE2014 cruise (**Supplementary Figs. 3 and 4, Supplementary Table 4).** A PERMANOVA from the main analysis confirmed that the site ($p = 0.001$ for Unifrac and W-Unifrac distances, Adonis2) and the life stage ($p = 0.001$, $p = 0.002$ for W-Unifrac and Unifrac distance, Adonis2) significantly influenced bacterial communities midgut tube whereas species only had a significant influence on bacterial communities with Unifrac distance ($p = 0.006$, Adonis2) (**Supplementary Table 3**). Similar results were observed with the second metabarcoding analysis on *R. exoculata* and *R. chacei* adult specimens from BICOSE2014 cruise (**Supplementary Table 4**).

Within the midgut tube, we focused on *Lachnospirales* identified in several studies in the digestive communities, only along the life stages of *Rimicaris* spp. [19, 23]. Moreover, *Lachnospirales* did not seem to colonize other symbiotic organs of *Rimicaris* spp. [19, 63], which suggest a specific role in the midgut tube. As shown in the barplot of Fig. 1 – displaying relative abundance of bacterial orders in each sample – *Lachnospirales* (here in pink) can represent between 0.08% to 51.98% of the relative abundance with 16 ASVs out of 833 (Table 3). Among all these ASVs, three being more represented: ASV72, ASV703 and ASV397 (**Supplementary Table 2)**. Even if not quantitative, the metabarcoding results indicate *Lachnospirales* presence in almost all specimens, and this lineage seemed to be the third most represented lineages together with *Ca. Microvillispirillaceae* (in light blue, mostly in subadults and adults) and *Campylobacterales* (in grey, mostly in juveniles) (Fig. 1, Table 3). *Lachnospirales* were almost not detected in *R. chacei* stage A juveniles, except in two out of five specimens from TAG (0.08% and 14.1% of the relative abundance) and one out of five from Snake Pit (7.4%). The results were more contrasted for *R. exoculata* stage A specimens. At Snake Pit (Table 3), two out of five *R. exoculata* stage A specimens were already colonized by *Lachnospirales*, up to 56% of the relative abundance for one specimen and 21% for the other, explaining the 15% average in Table 3. At TAG, *Lachnospirales* were not retrieved in only one out of five *R. exoculata* stage A specimens (but represented 6.6%, 0.02%, 6.6% and 1.2% for the others, Table 3). Some differences were also visible for older specimens (Fig. 1, Table 3). Indeed, only one out of five *R. chacei* subadult specimen from Snake Pit had *Lachnospirales* (0.4%), whereas four out of five subadult specimens from TAG harbored this bacterial lineage (38.2% for one specimen and the three others showing less than 1.5% of *Lachnospirales*). For *R. exoculata* older juveniles, *Lachnospirales* were present in almost all specimens. At TAG only one out of five stage B specimen (6.9%, 41.4%, 25.6% and 0.6% for other specimens), and one out of five subadult specimen (2.3%, 0.003%, 0.9% and 40.9% for other specimens) did not reveal *Lachnospirales* against 3 out of five stage B specimens from Snake Pit (Table 3). According to Fig. 1 and Table 3, R. *exoculata* adult specimens seemed to harbor more *Lachnospirales* living in dense aggregations while shrimps retrieved at the periphery seemed to be less colonized. In dense aggregations from Snake Pit, *R.*

exoculata were less colonized by *Lachnospirales* (four out of six specimens at Snake Pit against five out 6 specimens at TAG), leading to a more drastic decrease between specimens from dense aggregations and scattered individuals at TAG than Snake Pit (Fig. 1, Table 3). The second metabarcoding analysis focusing on adults, showed confirmed that *R. exoculata* from TAG were colonized by *Lachnospirales* like *R. chacei* specimens. However, the percentage of *Lachnospirales* within *R. chacei* adult midgut tube samples was very low, even close to 0% (**Supplementary Fig. 5, Supplementary Table 4).** Moreover, some differences were noticed between *R. exoculata* adult and *Rimicaris* spp juvenile specimens. Of note, the ASV397 (the third most abundant in samples, **Supplementary Table 2**) dominated mostly adult specimens. This was confirmed by ANCOM-BC (**Supplementary Table 5**) which showed that this ASV was less abundant in stage A juveniles (lfc= -2.33, padj = 0.032*), stage B juveniles (lfc = -2.29, padj = 0.040*) and subadult specimens (lfc = -2.48, padj = 0.012*) than in *R. exoculata* adult specimens. ASV17 from the metabarcoding analysis on *R. exoculata* and *R. chacei* adult specimens from BICOSE2014 cruise also highlighted differences between *R. exoculata* and *R. chacei* adult specimens. Of note, the ASV17 dominated *R. exoculata* specimens. This was confirmed by ANCOM-BC (lfc = 5.03, padj = 9.93e-05***) (**Supplementary Table 4**). According to the barplot observations (Fig. 1, **Supplementary Fig. 5**), a trend emerged between some lineages. Along the shrimp metamorphoses from juvenile A to adult stages, ASV related to *Campylobacteria* (*Campylobacterales* order) were less represented while those related to *Ca.* Microvillispirillaceae and *Lachnospirales* were more represented.

Table 3

Proportion of the main ASVs obtained and affiliated to Lachnospirales of the total of bacterial communities in the midgut tube samples of Rimicaris spp. specimens at different life stages (average ± standard deviation).

	R. chacei stage A	*R. chacei* subadult	*R. exoculata* stage A	*R. exoculata* stage B	*R. exoculata* subadult	*R. exoculata* adult	
						dense aggregation	scattered individuals
TAG							
Lachnospirales (% relative abundance)	2.83 ± 6.28 Per individual: 0%, 0.08%, 14.07%, 0%, 0%	8.18 ± 16.81 Per individual: 38.24%, 1.43%, 0.85%, 0%, 0.40%	2.91 ± 3.44 Per individual: 6.64%, 0%, 0.02%, 6.64%, 1.24%	14.91 ± 18.10 Per individual: 6.88%, 41.44%, 25.63%, 0.59%, 0%	8.73 ± 17.78 Per individual: 0%, 2.27%, 0.003%, 0.88%, 40.48%	34.48 ± 29.94 Per individual: 20.94%, 60.74%, 73.99%, 0%, 44.35%, 6.88%	0.07 ± 0.06 Per individual: 0%, 0.12%, 0.10%
Snake Pit							
Lachnospirales (% relative abundance)	1.48 ± 3.30 Per individual: 0%, 0%, 0%, 0%, 7.38%	0.08 ± 0.18 Per individual: 0%, 0.41%, 0%, 0%, 0%	15.27 ± 24.25 Per individual: 55.56%, 0%, 0%, 20.77%, 0%	12.37 ± 17.28 Per individual: 0%, 0%, 35.76%, 26.09%, 0%	27.39 ± 21.03 Per individual: 37.04%, 19.66%, 18.42%, 58.41%, 3.43%	11.98 ± 13.80 Per individual: 0%, 2.16%, 0%, 33.06%, 23.00%, 13.66%	7.43 ± 12.31 Per individual: 21.64%, 0%, 0.66%

Probe specificity and optimal hybridization

To complete the metabarcoding analyses and to show the distribution and representativeness of *Lachnospirales* in the midgut tube of adult and juvenile specimens, Fluorescent *in situ* Hybridization was done. First, we had to identify the *Lachnospirales* lineage within shrimp species through life stages by designing and optimizing a new specific probe.

To ensure the specificity of the new probe targeting *Lachnospirales*, Clostri-Lachno109, stringency tests (Table 2) were performed in the foregut and the midgut tube (**Supplementary Fig. 6**). Moreover, we used the cephalothorax of a *R. exoculata* subadult specimen as a negative control because *Lachnospirales* were never detected when using metabarcoding approaches

[23, 64]. According to the different tests, no hybridization was visible neither in the cephalothorax nor in the foregut and *Ca.* Microvillispirillaceae were not labelled with the new probe (**Supplementary Fig. 6A, B**). The optimal conditions to ensure the best specificity are a hybridization at 46°C for 3 hours with a buffer hybridization containing 30% formamide and a washing at 48°C for 15 minutes.

Distribution of *Lachnospirales* in the midgut tube

Based on previous studies [19, 23], *Lachnospirales* were expected to be localized in the midgut tube of both *R. chacei* and *R. exoculata* specimens. The use of the Clostri-Lachno109 specific probe confirmed their presence and restricted localization to the midgut tube of some specimens. Similar to *Ca.* Microvillispirillaceae, *Lachnospirales* were observed in the ectoperitrophic space, separated from the alimentary bolus by the peritrophic membrane. However, in contrast to *Ca.* Microvillispirillaceae, which are inserted between the epithelial microvilli [18], *Lachnospirales* were observed along the epithelium and without apparent integration between the microvilli (Fig. 2). Observations suggest they colonize the surface of the *Ca.* Microvillispirillaceae biofilm (or mixed with them) and the epithelium (Fig. 2B, D, E). According to the specimen and its midgut tube sections, two distinct morphotypes of *Lachnospirales* were observed. The first one comprised long and thin cells (about 0,5 µm in diameter *vs* for only 0,2 µm for *Ca.* Microvillispirillaceae), predominantly observed in stage B, subadult and adult *R. exoculata* specimens (Fig. 2B, C, D, F), with lower abundance in subadult and adult *R. chacei* specimens. The second consisted of coccobacilli, more frequently observed in *R. chacei* specimens (adults and subadults) and *R. exoculata* juveniles (Fig. 2A, E). FISH microscopy highlighted the fact that according to the specimen and the section hybridized, the abundance of *Lachnospirales* and *Ca.* Microvillispirillaceae varied. Indeed, in some sections, only one lineage was detected, whereas in others, both were present in different proportions (Fig. 2). These observations were in accordance with the patterns observed in the metabarcoding analyses. Indeed, *Lachnospirales* were observed from stage B to adult specimens of both species with limited detection in stage A (*R. exoculata*, one section among three individuals). Overall, substantial inter-individual and intra-gut variability in the relative abundance of both lineages was observed.

Metagenomic analyses

A novel symbiotic Lachnospirales family in the Rimicaris midgut tube

The two high-quality Metagenome-Assembled Genomes (MAGs) reconstructed from the midgut of adult *R. exoculata* specimens and collected from TAG (M_TAG_MAG_00001, 97.78% completeness & 0.1% redundancy) and Snake Pit (M_SnakePit_MAG_00001, 95.82% completeness & 0.14% redundancy) were affiliated with the order *Lachnospirales* [19]. These MAGs were closely related, sharing 97,28% ANI, consistent with assignment to the same species. Taxonomic classification using GTDB-Tk was limited to the order level (*Lachnospirales*) and both genomes were ultimately assigned to the CAMZNU01 family upon submission to GTDB. Both MAGs exhibited a relatively weak G + C content (from 28.52% to 28.56%) and a reduced genome size (about 1,5Mbp) compared to other *Lachnospirales* representatives. The order *Lachnospirales* clusters several families including the well described *Lachnospiraceae* family. This family comprises species with a genome G + C content ranging from 35% to 50% and a genome size between from 2,6 Mbp and 7,2 Mbp [65]. Two extremophiles *Lachnospiraceae* species - *Natranaerovirga pectinivora* and *N. hydrolytica* – isolated from hypersaline soda lakes, showed for example a G + C content about 32,27% and a genome size about 2,9 Mbp [66].

In the present study, the closest relatives to these new MAGs belong to the CAMVHY01 family harboring MAGs from sheep and mouse gut microbiota (Fig. 3) [67–69]. CAMVHY01 family showed similarities with both Snake Pit and TAG MAGs with a reduced genome size between 1,3 and 1,7Mbp, and a G + C content between 28.87% and 29.45%.

Energy and carbon metabolism of Lachnospirales

Both *Lachnospirales* MAGs harbor genes for the complete glycolysis pathway (EMP – Embden-Meyerhof-Parnas) similar to *Ca.* Microvillisprillaceae [19]. The main difference is that the phosphorylation of fructose-6-phosphate (F-6-P) to fructose-1,6-bisphosphate (F-1,6-BP), carried by PFK9 (K24182) in the latter, is carried by *pfkA* (K00850) in the *Lachnospirales* MAGs. A non-

oxidative pentose phosphate pathway was also identified in both MAGs with the addition of a transaldolase/glucose-6-phosphate isomerase (E.C.2.2.1.2, K13810) which is absent from *Ca.* Microvillisprillaceae (Fig. 4, **Supplementary Tables 6–8**). No complete Tricarboxylic acid (TCA) cycle was retrieved as only α-ketoglutarate dehydrogenase and fumarase were identified. However, the tripartite tricarboxylate transporter TctABC was detected, and could compensate for the level of lacking TCA cycle intermediates such as citrate, cis-aconitate or isocitrate [70]. We also focused on chitin degradation as in deep-sea environments, one of the most abundant sources of carbon is chitin [71]. The identification of carbohydrate-active enzyme (CAZyme) encoding genes revealed that both *Lachnospirales* MAGs harbor the *chiA* gene, encoding for chitinase. Chitinase would be exported out of the cell thanks to SecYEG system and SecA [72] (Fig. 4, **Supplementary Tables 6, 10–12,14**). In addition to chitinase secretion, our MAGs also harbored Phosphotransferase System (PTS) machinery and NagE transporter allowing the entrance of GlcNAc into the cell and the NgcEFG transporter which could be involved in chitobiose import [73]. As *Ca.* Micovillispirillaceae, both MAGs encoded genes involved in chitobiose and GlcNAc-6P degradation (respectively *nagZ* and *nagA*). The GlcNac-6P contributes to the bacterial wall cell synthesis. It must be deacetylated to participate in the peptidoglycan layer formation (several genes involved in this process have been retrieved, **Supplementary Tables 6, 9–12,14**) [74]. Therefore, both *Lachnospirales* MAGs harbor all the genetic material necessary for chitin degradation and recycling as well as synthesis of the bacterial cell wall. Both MAGs showed genes coding for another PTS associated transporter: *murP* and *crr* encode for translocation of N-acetyl-muramic acid (MurNAc) which is also a component of peptidoglycan. Surprisingly, no other sugar transporter was found except for xylose.

In deep-sea hydrothermal vents, many microorganisms, moreover symbiotic ones, rely on autotrophic chemosynthesis to ensure primary carbon organic synthesis. However, none of the two MAGs harbors genes for a complete CBB cycle and key genes coding the RuBisCo for example are absent (Fig. 4). Interestingly, even if these MAGs could not fix CO_2 using the CBB cycle, they could be able to fix CO_2 in two secondary pathways. First, they could perform an anapleurotic reaction transforming pyruvate into oxaloacetate and fixing CO_2 using a pyruvate carboxylase (encoded by *pycB* gene, K01960) [75]. Secondly, the gene *por* (K03737) coding for a Pyruvate:ferredoxin oxidoreductase [76] is also involved in the carboxylation of acetyl-CoA into pyruvate, which requires a molecule of CO_2 (Fig. 4, **Supplementary Tables 6–8**). In contrast to *Ca.* Microvillispirillaceae, both MAGs seemed to harbor a basic aerobic respiratory chain where the proton pumping NADH:ubiquinone oxidoreductase respiratory complex I is encoded by *ndh* and the cytochrome *bd* ubiquinol oxidase SU I & II (encoded by *cydA* and *cydB* genes) is using O_2 as the terminal electron acceptor of the respiratory chain. However, in M_SnakePit_MAG_00001, a second source of energy might come from the oxidation of dihydroorotate, which could be carried by the dihydroorotate dehydrogenase (DODH) encoded by *pyrD* (class II) which is located in the membrane [77]. This enzyme can subsequently reduce quinones from the respiratory chain. The presence of this mechanism could be useful to counteract the lack of NADH production since the TCA cycle is incomplete. Furthermore, we also detected the presence of *pyrD* (class I) and *pyrK*, suggesting the subsequent oxidation of dihydroorotate and reduction of NAD + into NADH, H+. In the same way, 3 out of the 4 genes encoding for the Hnd dehydrogenase could also be involved in NADH replenishment while oxidizing H_2 [78, 79] (Fig. 4, **Supplementary Tables 6, 9–12**).

Amino acid and vitamin synthesis and transporters

Only two amino acid biosynthesis pathways were identified in both *Lachnospirales* MAGs. While the lysine biosynthesis pathway (module M00527) was present, the key gene encoding for LL-diaminopimelate aminotransferase (K10206) was absent (**Supplementary Tables 6–8**). Glutamate could also be synthesized by degrading histidine (M00045), but no transporter involved in histidine intake nor pathway for histidine synthesis was detected. Furthermore, polyamine biosynthesis such as putrescine and spermidine were retrieved. These components, known to be involved in biofilm formation and oxidative stress resistance, might have a role in the colonization of the ectoperitrophic space [80–82]. The small number of complete amino acid biosynthesis pathways could be compensated by the entrance of oligopeptides and dipeptide through ABC transporters such as Opp (*oppD* & *oppF*) and Dpp (*dppB*) respectively. No complete vitamin biosynthesis pathways were found (**Supplementary Tables 6–12**). The vitamin intake may come from the outside, like biotin. The presence of biotin ABC transporters genes suggests the intake of this vitamin, but no other vitamin transporter was detected (**Supplementary Table 6–12**).

Mobility, chemotaxis and secretion systems

Genes involved in flagellum biosynthesis were also investigated. Indeed, the flagella is involved in host recognition and colonization by its symbionts [83]. It allows the cell to move towards host organs before infestation and attachment. Both MAGs showed about thirty genes coding for flagellum biosynthesis (**Supplementary Tables 6, 9–12**). In addition to core flagellar components, genes encoding for Type IV pili were also detected (*pilB*, *pilC*, *pilT*), suggesting a potential for twitching mobility and in adhesion/fixation to eukaryotic surface.

Chemotaxis-related genes were then examined in relation to flagellar mobility, which are considered essential for attraction and host adaptation. Chemotaxis consists in molecular signal detection, which, depending on their nature (attractants or repellents) sends a message to the flagellum and acts on its rotary direction. Unlike *Ca.* Microvillispirillaceae which encodes a complete chemotaxis pathway [19], both *Lachnospirales* MAGs only harbor the CheY protein. They also had only two genes encoding for a type II secretion system. These chemotaxis and type II secretion genes could have been lost during assembly. Furthermore, we observed genes encoded for a SecYEG system but no Tat system.

Immunity system

In this study, both *Lachnospirales* MAGs harbor genes encoding for the immune system. Especially, CRISPR-Cas system genes were identified in 3 contigs (M_ SnakePit_MAG_00001_000000059859, M_ SnakePit_MAG_00001_000000041930, M_ SnakePit_MAG_00001_000000031594) containing respectively 23, 14 and 6 spacers for M_SnakePit_MAG_00001, and in 2 contigs (M_TAG_MAG_00001_000000006514 and M_TAG_MAG_00001_000000007976) with both 8 spacers for M_TAG_MAG_00001. In addition, several *cas* genes were detected in M_ SnakePit_MAG_00001 on contig M_ SnakePit_MAG_00001_000000041930: *cas1* Type II, *cas2* Type I, II and III and *cas3* Type I [84] (**Supplementary Table 6, 9–13**).

Cell division and morphology

In this study, two distinct morphotypes of *Lachnospirales* cells were observed: coccobacilli shape and long filamentous cells (Fig. 2). When in filamentous form, *Lachnospirales* closely resembled *Ca.* Microvillispirillaceae previously described as long single-cell filamentous bacteria [18, 20, 21]. Aubé et al., 2022 [19] also demonstrated that *Ca.* Microvillispirillaceae harbor all the cell division machinery without dividing themselves. *Lachnospirales* morphology suggested a similar non-dividing lifestyle. To investigate it, chromosome staining was performed using YOYO^{TM}-1 dye (Fig. 5). Fluorescence microscopy revealed that filamentous cells did not undergo septation despite exhibiting multiple replicated chromosome copies within a single cell (Fig. 5B, C, D.). These observations remind those of Aubé et al., 2022 [19], which led us to focus on genes involved in cell cycle processes. Both MAGs contained the genes for DNA replication, those for Z-ring formation and protease, suggesting ability for replication and division.

Discussion

Acquisition and transmission of *Lachnospirales*

This study revealed that *Lachnospirales* were mostly detected in the midgut tube of later juvenile stages (Stage B and subadult) of both *Rimicaris species* and *R. exoculata* adults, particularly in adult individuals from dense aggregations (Fig. 1, Table 3). In contrast, only a few stage A juveniles from both species from Snake Pit exhibited colonization (more contrasted at TAG), suggesting a symbiotic acquisition post-installation on site. The sporadic detection of *Lachnospirales* in some stage A individuals may be explained by the continuous development of the host. *Rimicaris* juveniles undergo metamorphosis until they reach adult size but the molts number required for complete metamorphosis remains unknown. Therefore, individuals classified morphologically as stage A may, in some cases, be developmentally closer to stage B, potentially accounting for the presence of more established symbiotic populations [23]. As in the case of *Ca.* Microvillispirillaceae, the transmission of this lineage remains unclear [19]. Indeed, during the BICOSE2 cruise, environmental water samples were collected and analyzed. Analyses revealed that almost neither *Lachnospirales* nor *Ca.* Microvillispirillaceae were detectable in the surrounding environment [85,

86] rejecting the hypothesis of a strict horizontal transmission. Yet, the lack of *Lachnospirales* in almost all early-stage A is also in disfavor of a strict vertical transmission hypothesis. Here we rather suggest a mixed horizontal transmission as hypothesized in Guéganton et al., 2024 [23]. Symbionts may be evacuated by older specimen's feces and then inoculate juveniles in the close environment. This hypothesis may also explain the lack of *Lachnospirales* in almost all *R. chacei* juvenile and adult specimens. Because *R. chacei* juveniles live in nurseries isolated from adult aggregations [29, 31], the symbionts acquisition may then become hazardous depending on acquisition of bacteria being scattered by the water current.

Metabarcoding analyses also revealed that scattered individuals were less or not colonized by *Lachnospirales* (Fig. 1, Table 3). These results suggest that *Lachnospirales* tend to decrease when the host resides in a more oxygenated microhabitat. Yet, to confirm this hypothesis, further research and experimentation should be carried out (host exposure time, physico-chemical conditions…).

Chitin degradation

Lachnospirales may assist their host to degrade and recycle chitin, producing nutrients for the host and improving its fitness, but may also be involved in bacterial syntrophy. Arthropods like *R. exoculata* and *R. chacei* are encased in an exoskeleton mostly composed of chitin, a complex polymer. They are submitted to molt and must synthetize *de novo* their cuticle. During the molt process, the host secretes a chitinase that allows the old cuticle lysis while synthesizing the new one [87]. For *R. exoculata*, this molt cycle duration is about 10 days, leading to an important cost of energy and nutrients requirements [88]. This short cycle may suggest the presence of an exterior partner to help the shrimp during this energy requirement period. Chitin is a complex insoluble polymer (β1,4-linked N-acetylglucosamine- GlcNAc) that cannot enter microbial cells for degradation. First, a secreted chitinase (such as endochitinase or exochitinase) must degrade chitin in smaller polymers that can then enter microbial cells [89]. Aubé et al., 2022 [19] showed in their study that *Ca.* Micovillispirillaceae had several Phosphotransferase System transporters such as *chbB,C,A* and *nagE*. These transporters may allow final chitin recycling by importing chitobiose (a dimer of N-acetyl-D-glucosamine resulting from chitin degradation) and N-acetyl-D-glucosamine (GlcNAc, final sub-unit of chitobiose) into the bacterial cells. However, only chitinase from family 19 Glycoside Hydrolase (GH19) was found, suggesting another lineage would help the host chitinase to degrade chitin during molt. In fact, chitinases from family GH19 are less retrieved in bacteria and their function remains unclear, suggesting they are not capable degrading completely crystalline chitin [90]. On the contrary, the presence of chitinase from family GH18– majority found in bacteria and characterized as essential for chitin degradation [91] - land its secretion related genes in the bacterial *Lachnospirales* cell genome suggest a potential support to the host to degrade its chitin quickly and to reduce its energetic cost. *Ca.* Microvillispirillaceae was hypothesized to use GlcNAc to produce F6P and synthesize cell wall since they possess the genes involved in these pathways together with those for chitobiose and GlcNAc transport into the cell [19]. They may then rely on *Lachnospirales* chitinase activity to ensure their full metabolic functioning. This bacterial syntrophy may also be involved in amino acids and vitamins exchange. Indeed, *Lachnospirales* could not synthesize vitamins and produce different amino acids than *Ca.* Microvillispirillaceae. Consequently, each lineage could provide to the other the metabolic products they rely on.

Metabolism

Contrary to main symbiotic lineages from the cephalothorax cavity harboring CBB cycle or rTCA cycle to synthetize primary organic compounds [63, 92], *Lachnospirales* are devoid of those. Mainly heterotrophic, they rely on their host and other microorganisms to ensure their nutrition. However, in this study, two secondary CO_2 fixation pathways were identified. Consequently, *Lachnospirales* symbionts of *R. exoculata* may be able of mixotrophy, even if the heterotrophic pathway may still dominate.

A particularly intriguing finding from this study is the stable co-occurrence of two bacterial lineages in the midgut of *Rimicaris*: the anaerobic *Ca. Microvillispirillaceae* and the presumably microaerophilic *Lachnospirales*. Indeed, *Ca.* Microvillispirillaceae are inserted between the microvilli of the epithelial cells within the ectoperitrophic space, a usually sterile zone for decapods [19, 22], whereas in this study, *Lachnospirales* appeared to colonize the epithelial surface without penetrating between the microvilli (Fig. 1). Consequently, *Lachnospirales* mostly cover the epithelium as their co-occurring bacteria, suggesting they

could pick up O_2 leading to its decrease in the microvilli area. Therefore, *Ca.* Microvillispirillaceae would not be in contact with O_2 explaining their co-occurrence with *Lachnospirales*.

A potential host control

As observed for *Ca.* Microvillispirillaceae, *Lachnospirales* symbionts appear not to undergo cell division, harboring long cells shape morphology [19] and both symbionts are located in a zone described as “sterile” for decapods. This long cell shape morphology had been retrieved in *Candidatus Arthromitus*, members of *Lachnospiraceae*, found in arthropods guts [91] but still undergo cell division. Consequently, a potential explanation for *Rimicaris*' case is that the host prevents and controls its symbiont's cell division, but not their chromosomal replication, resulting to long and thin multichromosomic filamentous symbionts. Further investigation should be conducted to understand the mechanisms involved in this control. Cell division is regulated by the protein FtsZ within the Z-ring. The inhibition of this protein may lead to the apparition of long and single filamentous bacteria. This can be caused by small molecules playing as antibiotics or having antimicrobial activities (Berberine, cinnamaldehyde…) [94–96]. In some trypanosomatid protozoa regulating their endosymbiont cycle, it has been shown that a perturbation in the host metabolism by specific proteins cause a bacterial cell elongation and cell division arrest [97]. Consequently, we could suppose that *Rimicaris* spp. may produce some specific molecules in their digestive system, such as AMPs (Anti-Microbial Peptides), as the one retrieved in their cephalothorax [98].

According to the metagenomic analyses, *Lachnospirales* lack genes encoding chemotaxis. The presence of flagellum and Type IV Pili would also facilitate their recognition and adhesion, but additional mechanisms may be implied in host and together with other recognition molecules.

Immunity system: a key point along the sea-land continuum

A previous study reported a striking imbalance between the number of juveniles and adults *Rimicaris chacei*, with high juvenile abundance but markedly fewer adults, suggesting a population collapse during initial metamorphosis [31]. This collapse may be also explained by the low colonization of *Lachnospirales* in juveniles. In fact, because *Lachnospirales* cover the epithelium and *Ca.* Microvillispirillaceae cells, they may play a protective barrier role separating the epithelium and *Candidatus* Microvillispirillaceae from the peritrophic membrane and the alimentary bolus.

Their putative defensive role may be also reinforced by the presence of a CRISPRs/*cas* complex usually involved in immunity whereas *Candidatus* Microvillispirillaceae only harbor CRISPRs suggesting an incomplete immune system [19]. With this “barrier” role and their immunity genes, *Lachnospirales* might have a significant role in the holobiont protection. Their immune potential may be similar to other *Lachnospirales* ones found in humans and rodents [26, 27]. These symbiotic bacteria can degrade complex carbohydrates like cellulose acting as an intestinal barrier [27]. A study showed that *Lachnospiraceae* produce butyric acid, involved in human host digestive system protection from colon cancer [99, 100]. *Lachnospiraceae* symbionts have been detected as great potential candidates for intestinal therapeutics. For example, *Lachnospiraceae* bacterium MA2020 harbors *Cas12a* ortholog that has been mutated, increasing its cleavage efficiency [101, 102]. Without these symbionts, the digestive microbiota of the host may be more exposed to potential threats such as bacteria or viruses, leading to intestinal dysbiosis.

Another stinking point of this study is that *Lachnospirales* and *Ca.* Microvillispirillaceae (*Deferribacteres* order) closest relatives are both retrieved in the digestive system of terrestrial mammals. In fact, the CAMVHY01 family (closest relative to *Lachnospirales* MAGs of this study) [68, 69] and *Mucispirillum* sp. [103, 104] (closest relative to *Ca.* Microvillispirillaceae) are found in murine gut microbiota. *Mucispirillum schaedleri*, that colonize the murine gut mucus, protect the epithelium cells from pathogens (like *Salmonella enterica* serovar Typhimurium colitis that can cause severe host diseases [105]) and are a protective barrier against the alimentary bolus content. Their implication in the immune system of the host seems similar to the one of *Ca.* Microvillispirillaceae as described in Guéganton, et al., 2022 and Aubé et al., 2022 [18, 19]. For both hosts, they are inserted between the microvilli of the midgut tube epithelium cells and share the presence of CRISPRs. CAMVHY01 family and *Lachnospiraceae* colonize as well murine gut microbiota [68, 69] and may be implied in the host immunity [26, 27, 99, 100].

Therefore, *Lachnospirales* and *Deferribacteres* being retrieved into the same ecological niches of different hosts reinforces the hypothesis they may be syntrophic lineages.

Moreover, for *Lachnospirales*, some relatives have been found in mammals like cattle, rodents like mice and chinchillas or human digestive system. This lineage can thus colonize aquatic and terrestrial hosts, supporting the importance of the eukaryotic evolution along the land-sea continuum. To go further in the comprehension of the evolution of *Lachnospirales* between aquatic and terrestrial hosts, it could be interesting to detail and compare the metabolism of CAMVHY01 family located in mouse and cattle gut.

New candidate names

According to our MAG functional and phylogenomic analyses as well as cell observations, we propose new candidate names for this novel *Lachnospirales* family. We propose here a new fam. nov., gen. nov. and genus sp. nov. for the novel family represented by these MAGs. We propose the new family *Candidatus* Syntrospirillaceae, named this way because they are long and thin bacteria since they do not seem to divide themselves. Then, we propose the new genus *Candidatus* Rimicarisintestine, according to its location in the *Rimicaris* spp. midgut tube. Then the species name proposed is *Candidatus* Rimicarisintestine chitinovorans due to their potential in chitin degradation.

Conclusion

The discovery of a novel symbiotic relationship in the midgut tube of *Rimicaris* shrimp with key enzymes for complex polymer degradation and immune functional genes suggests complex interactions within the holobiont. Moreover, these interactions open the way to new questions regarding syntrophy between symbionts. Indeed, *Lachnospirales* and *Candidatus* Microvillispirillaceae may communicate, first to avoid competition and then to complement their nutritional requirements. It also reveals that the holobiont can adapt itself to environmental conditions, suggesting a regulation of its symbiotic communities. It could be interesting to take our research a step further, by analyzing the host genome or using metabolomic approaches that would help us to understand the overall functioning of the holobiont. Even if our research progresses, there's still a long way to go before we fully understand the full extent of this holobiont's functioning and interactions. Indeed, according to Aubé et al., 2022 [19], no MAG of *Lachnospirales* was retrieved in specimen's midgut tube from Rainbow (36°13' N—33°54' W, 2300 m depth), suggesting the non-universality of this symbiont. Consequently, the question of universality remains open, suggesting depth (Rainbow and Puy des Folles being shallower) or geochemical environments (Rainbow and HYDRA fluids being enriched in hydrogen and methane) may have an impact on the holobiont composition. Further studies on *R. exoculata* specimens from Rainbow, Puy des Folles (20°30' N—45°38' W, 2000 m depth) and Hydra (24°96' N—45°57' W, 3700 m depth) sites should be carried to answer this question.

Declarations

Acknowledgments

We thank cruise the chief scientists of, BICOSE2014, BICOSE2 and HERMINE cruises (M.A. Cambon, Yves Fouquet) as well as the captains and crews of R/V *Pourquoi pas*?, HOV Nautile and ROV ViCTOR 6000 for their contribution in collecting samples. We also thank the sequencing platform (the INRAe GeT-PlaGE plateform—Genotoul, Castanet-Tolosan, France, project Rimi-life). We thank P. Elies and the Plateform of Imaging and Measures in Microscopy (PIMM) at the Université de Bretagne Occidentale (UBO) for the acquisitions using the confocal microscope. We thank Cyril Noël and the SEBIMER platform for their technical support and the sequences deposited in ENA. We also thank Ouafae Rouxel for her device and the different adult slides she gave to realize FISH experiments. To finish, we thank Vincent Apremont for the data acquisition.

Authors' contributions

MG performed the conception, the data acquisition and analysis, the laboratory assays, interpreted the data and wrote the manuscript. LA performed the data analysis, interpreted the data and wrote the manuscript. JA, VCG and LD revised the

manuscript. JA and VCG performed the data acquisition. MAC managed the project, interpreted the data and wrote the manuscript. The authors read and approved the manuscript.

Funding

This work was supported by Ifremer REMIMA program and LIFEDEEPER France 2030 ANR-22-POCE-0007, Ifremer—Région Bretagne and UBO for Marion Guéganton fellowship.

Competing Interests

The authors declare no conflicts of interest.

Ethics approval and consent to participate

Not applicable

Consent for publication

Not applicable

Authors' information

MG new affiliation since September 1st 2025 : Univ Rouen Normandie, Univ Caen Normandie, CNRS, M2C, UMR 6143, Rouen, France.

References

1. *Dubilier, N., Bergin, C., Lott, C. 2008. "Symbiotic diversity in marine animals: The art of harnessing chemosynthesis." Nat Rev Microbiol, 6(10):725–40. https://doi.org/10.1038/nrmicro1992.*
2. *Zilber-Rosenberg, I., and E. Rosenberg. 2008. "Role of Microorganisms in the Evolution of Animals and Plants: The Hologenome Theory of Evolution." FEMS Microbiology Reviews, 32: 723–735. https://doi.org/10.1111/j.1574-6976.2008.00123.x*
3. *Sogin, E. M., M. Kleiner, C. Borowski, H. R. Gruber-Vodicka, and N. Dubilier. 2021. "Life in the Dark: Phylogenetic and Physiological Diversity of Chemosynthetic Symbioses." Annual Review of Microbiology, 75: 695–718.*
4. *Zook, D. 2015. "Symbiosis-Evolution's Co-Author." Reticulate Evolution, ed. N. Gontier (Springer US). 41-81. Doi:10.1007/978-3-319-16345-1_2*
5. *McFall-Ngai, M. J. 2002 "Unseen forces: the influence of bacteria on animal development." Dev Biol., 242:1–14.*
6. *Bordenstein, S. R., Thei,s K. R. 2015. "Host biology in light of the microbiome: ten principles of holobionts and hologenomes". PLoS Biol., 13:e1002226. Public Library of Science.*
7. *Nussbaumer, A. D., C. R. Fisher, and M. Bright. 2006. "Horizontal Endosymbiont Transmission in Hydrothermal Vent Tubeworms." Nature, 441: 345–348. https://doi.org/10.1038/nature04793.*
8. *Duperron, S. 2010. "The Diversity of Deep-Sea Mussels and Their Bacterial Symbioses." The Vent and Seep Biota edited by S.Kiel, 33: 137–167. Dordrecht, The Netherlands: Springer Netherlands.*
9. *Suzuki, Y., Takai, K., Tsuchida, S., Kojima, S., Watanabe, H., Utsumi, T., et al. 2006. "Host-Symbiont Relationships in Hydrothermal Vent Gastropods of the Genus Alviniconcha from the Southwest Pacific." Appl. Environ. Microbiol., 72. doi:10.1128/aem.72.2.1388-1393.2006.*
10. *Williams, A. B., and P. A. Rona. 1986. "Two New Caridean Shrimp (Bresiliidae) From a Hydrothermal Field on the Mid-Atlantic Ridge." Journal of Crustacean Biology, 6: 446–462. https://doi.org/10.1163/193724086X00299.*
11. *Zbinden M., Cambon-Bonavita M.-A. 2020. « Rimicaris exoculata: biology and ecology of a shrimp from deep-sea hydrothermal vents associated with ectosymbiotic bacteria." Mar Ecol Prog Ser., 652:187–222.*

12. *Gebruk, A. V., E. C. Southward, H. Kennedy, and A. J. Southward. 2000. "Food Sources, Behaviour, and Distribution of Hydrothermal Vent Shrimps at the Mid-Atlantic Ridge." Journal of the Marine Biological Association of the United Kingdom, 80: 485–499. https://doi.org/10.1017/S0025315400002186.*
13. *Ponsard, J., M.-A. Cambon-Bonavita, M. Zbinden, et al. 2013. "Inorganic Carbon Fixation by Chemosynthetic Ectosymbionts and Nutritional Transfers to the Hydrothermal Vent Host-Shrimp Rimicaris exoculata." ISME Journal, 7: 96–109.*
14. *Methou, P., L. Michel, M. Segonzac, M.-A. Cambon-Bonavita,and F. Pradillon. 2020. "Integrative Taxonomy Revisits the Ontogeny and Trophic Niches of Rimicaris Vent Shrimp." Royal Society Open Science, 7:200837. https://doi.org/10.1098/rsos.200837.*
15. *Casanova, B., M. Brunet, and M. Segonzac. 1993. "Impact of Bacterial Epibiosis on Functional Morphology of Shrimp Associated With the Mid-Atlantic Hydrothermal Conditions." Cahiers de Biologie Marine, 34:573–588.*
16. *Apremont, V., M.-A. Cambon-Bonavita, V. Cueff-Gauchard, et al. 2018. "Gill Chamber and Gut Microbial Communities of the Hydrothermal Shrimp Rimicaris chacei Williams and Rona 1986: A Possible Symbiosis." PLoS One, 13: e0206084. Doi : 10.1371/journal.pone.0206084.*
17. *Polz, M. F., Robinson, J. J., Cavanaugh, C. M., Van Dover, C. L. 1998. "Trophic ecology of massive shrimp aggregations at a mid-Atlantic ridge hydrothermal vent site." Limnol Oceanogr.,43:1631–8.*
18. *Guéganton, M., O. Rouxel, L. Durand, et al. 2022. "Anatomy and Symbiosis of the Digestive System of the Vent Shrimp Rimicaris exoculata and Rimicaris chacei Revealed Through Imaging Approaches." Frontiers in Marine Science 9: 903748. https://doi.org/10.3389/fmars.2022.903748.*
19. *Aubé, J., M.-A. Cambon-Bonavita, L. Velo-Su.rez, et al. 2022. "A Novel and Dual Digestive Symbiosis Scales Up the Nutrition and Immune System of the Holobiont Rimicaris exoculata." Microbiome, 10: 189. https://doi.org/10.1186/s40168-022-01380-2.*
20. *Durand, L., Zbinden, M., Cueff-Gauchard, V., Duperron, S., Roussel, E. G., Shillito, B., et al. 2009. "Microbial diversity associated with the hydrothermal shrimp Rimicaris exoculata gut and occurrence of a resident microbial community." FEMS Microbiol Ecol.,71:291–303.*
21. *Durand, L., Roumagnac, M., Cueff-Gauchard V., et al. 2015. "Biogeographical Distribution of Rimicaris exoculata Resident Gut Epibiont Communities Along the Mid-Atlantic Ridge Hydrothermal Vent Sites." FEMS Microbiology Ecology, 91: 1–15. https://doi.org/10.1093/femsec/fiv101.*
22. *Martin, G. G., Z. Natha, N. Henderson, S. Bang, H. Hendry, and Y. Loera. 2020. "Absence of a Microbiome in the Midgut Trunk of Six Representative Crustacea." Journal of Crustacean Biology 40: 122–130. https://doi.org/10.1093/jcbiol/ruz087.*
23. *Guéganton, M., Methou, P., Aubé, J., Noël, C., Rouxel, O., Cueff-Gauchard, V. et al. 2024. " Symbiont acquisition strategies in post-settlement stages of two co-occuring deep-sea Rimicaris shrimp." Ecology and Evolution. 14e70369. https://doi.org/10.1002/ece3.70369.*
24. *Zou, Y., Liang, N., Zhang, X., Han, C., and Nan, X. 2021. "Functional differentiation related to decomposing complex carbohydrates of intestinal microbes between two wild zokor species bases on 16SrRNA sequences." BMC Veterinary Research, 17:216. https://doi.org/10.1186/s12917-021-02911-z*
25. *Li, M., Zhao, Y., Wang, Y., Geng, R., Fang, J., Kang, S.-G. et al. 2022. "Eugenol, a major component of clove oil, attenuates adiposity, and modulates gut microbiota in high-fat diet-fed mice." Mol. Nutr. Food Res., 66: 2200387. Doi: 10.1002/mnfr.202200387.*
26. *Wu, Y., Liu, B., Ma, X., Yang, L., Lu, X., Wang, W. et al.2024. "The microbiota architecture of the chinchilla gastrointestinal tract." Veterinary Sciences, 11:58. https//doi.org/10.3390/vetsci11020058.*
27. *Vacca, M., Celano, G., Calabrese, F. M., Porincasa, P., Gbbetti, M., De Angelis, M. 2020. "The controversial role of human gut Lachnospiraceae." Microorganisms, 8 ;573. Doi: 10.3390/microorganisms8040573.*
28. *Breusing, C., Osborn, K. J., Girguis, P. R., and Reese, A. T. 2022. "Composition and metabolic potential of microbiomes associated with mesopelagic animals from Monterey Canyon." ISME. Doi: 10.1038/s43705-022-00195-4*
29. *Hernández-Ávila, I., M.-A. Cambon-Bonavita, J. Sarrazin, and F. Pradillon. 2022. "Population Structure and Reproduction of the Alvinocaridid Shrimp Rimicaris exoculata on the Mid-Atlantic Ridge: Variations Between Habitats and Vent Fields."*

Deep-Sea Research Part I, 186: 103827. https://doi.org/10.1016/j.dsr.2022.103827.

30. *Pond, D. W., A. Gebruk, E. C. Southward, et al. 2000. "Unusual Fatty Acid Composition of Storage Lipids in the Bresilioid Shrimp Rimicaris exoculata Couples the Photic Zone With MAR Hydrothermal Vent Sites." Marine Ecology Progress Series 198: 171–179. https://doi.org/10.3354/meps198171.*
31. *Methou, P., I. Hernández-Ávila vila, C. Cathalot, M.-A. Cambon-Bonavita, and F. Pradillon. 2022. "Population Structure and Environmental Niches of Rimicaris Shrimp From the Mid-Atlantic Ridge." Marine Ecology Progress Series, 684: 1–20. https://doi.org/10.3354/meps13986.*
32. *Bright, M., and S. Bulgheresi. 2010. "A Complex Journey: Transmission of Microbial Symbionts." Nature Reviews. Microbiology, 8: 218–230. https://doi.org/10.1038/nrmicro2262.*
33. *Wentrup, C., A. Wendeberg, M. Schimak, C. Borowski, and N. Dubilier. 2014. "Forever Competent: Deep-Sea Bivalves Are Colonized by Their Chemosynthetic Symbionts Throughout Their Lifetime." Environmental Microbiology, 16: 3699–3713. https://doi.org/10.1111/1462-2920.12597*
34. *Charlou, J. L., Donva, J. P., Konn, C., Ondréas, H., Fouquet, Y., Jean-Baptiste, P., et al. 2010. "High production and fluxes of H2 and CH4 and evidence of abiotic hydrocarbon synthesis by serpentinization in ultramafic-hosted hydrothermal systems on the mid-Atlantic ridge." Diversity of hydrothermal systems on slow spreading ocean ridges: American Geophysical Union (AGU); p. 265–96.*
35. *Helermann, D. P. R., M. Labrenz, K. Jürgens, S. Bertilsson, J. J. Waniek, and A. F. Andersson. 2011. "Transitions in Bacterial Communities Along the 2000 Km Salinity Gradient of the Baltic Sea." ISME Journal, 5:1571–1579. https://doi.org/10.1038/ismej.2011.41.*
36. *Chklovski, A., Parks, D. H., Woodcroft, B. J., and Tyson, G. W. 2023. "CheckM2: a rapid, scalable and accurate tool for assessing microbial genome quality using machine learning." Nature Methods, 20(8): 1203-1212.*
37. *Jain, C., Rodriguez-R, L. M., Phillippy, A. M., Konstantinidis, K. T., & Aluru, S. 2018. "High throughput ANI analysis of 90K prokaryotic genomes reveals clear species boundaries." Nature communications, 9(1) : 5114.*
38. *Chaumeil, P. A., Mussig, A. J., Hugenholtz, P., and Parks, D. H. 2022. "GTDB-Tk v2: memory friendly classification with the genome taxonomy database." Bioinformatics, 38(23) : 5315-5316.*
39. *Capella-Gutiérrez, S., Silla-Martínez, J. M., and Gabaldón, T. 2009. "trimAl: a tool for automated alignment trimming in large-scale phylogenetic analyses." Bioinformatics, 25(15): 1972-1973.*
40. *Minh, B. Q., Schmidt, H. A., Chernomor, O., Schrempf, D., Woodhams, M. D., Von Haeseler, A., and Lanfear, R. 2020. "IQ-TREE 2: new models and efficient methods for phylogenetic inference in the genomic era." Molecular biology and evolution, 37(5): 1530-1534.*
41. *Seemann, T. 2014. "Prokka: rapid prokaryotic genome annotation." Bioinformatics, 30(14) : 2068-2069.*
42. *Eren, A. M., Kiefl, E., Shaiber, A., Veseli, I., Miller, S. E., Schechter, M. S., et al. 2021. "Community-led, integrated, reproducible multi-omics with anvi'o." Nature microbiology, 6(1): 3-6.*
43. *Vallenet, D., Calteau, A., Dubois, M., Amours, P., Bazin, A., Beuvin, M., et al. 2020. "MicroScope: an integrated platform for the annotation and exploration of microbial gene functions through genomic, pangenomic and metabolic comparative analysis." Nucleic acids research, 48(D1): D579-D589.*
44. *Zheng, J., Ge, Q., Yan, Y., Zhang, X., Huang, L., & Yin, Y. 2023. "dbCAN3: automated carbohydrate-active enzyme and substrate annotation." Nucleic Acids Research, 51(W1): W115-W121.*
45. *Di Tommaso, P., M. Chatzou, E. W. Floden, P. P. Barja, E. Palumbo, and C. Notredame. 2017. "Nextflow Enables Reproducible Computational Workflows." Nature Biotechnology, 35: 316–319. https://doi.org/10.1038/nbt.3820.*
46. *Bolyen, E., J. R. Rideout, M. R. Dillon, et al. 2019. "Reproducible, Interactive, Scalable and Extensible Microbiome Data Science Using QIIME 2." Nature Biotechnology, 37: 852–857. https://doi.org/10.1038/s41587-019-0209-9.*
47. *Martin, M. 2011. "Cutadapt removes adapter sequences from high-throughput sequencing reads." EMBnet.journal, 17 (3).*
48. *Sasada, R., Weinstein, M., Prem, A., Jin, M., Bhasin, J. 2020. "FIGARO: An efficient and objective tool for optimizing microbiome rRNA gene trimming parameters." Journal of Biomolecular Techniques : JBT, 31 (S2).*

49. *Callahan, B. J., P. J. McMurdie, M. J. Rosen, A. W. Han, A. J. A. Johnson, and S. P. Holmes. 2016. "DADA2: High-Resolution Sample Inference From Illumina Amplicon Data." Nature Methods, 13: 581–583. https://doi.org/10.1038/Nmeth.3869.*
50. *Olesen, S. W., C. Duvallet, and E. J. Alm. 2017. "dbOTU3: A New Implementation of Distribution-Based OTU Calling." PLoS One, 12:e0176335. https://doi.org/10.1371/journal.pone.0176335.*
51. *McKnight, D. T., R. Huerlimann, D. S. Bower, L. Schwarzkopf, R. A. Alford, and K. R. Zenger. 2019. "MicroDecon: A Highly Accurate Read-Subtraction Tool for the Post-Sequencing Removal of Contamination in Metabarcoding Studies." Environmental DNA, 1: 14–25. https://doi.org/10.1002/edn3.11.*
52. *Quast, C., E. Pruesse, P. Yilmaz, et al. 2013. "The SILVA Ribosomal RNA Gene Database Project: Improved Data Processing and Web-Based Tools." Nucleic Acids Research, 41: D590–D596.*
53. *Lin, H., and S. D. Peddada. 2020. "Analysis of Compositions of Microbiomes With Bias Correction." Nature Communications, 11: 3514. https://doi.org/10.1038/s41467-020-17041-7.*
54. *Love, M. I., Huber, W., Anders, S. 2014. "Moderated estimation of fold change and dispersion for RNA-seq data with DESeq2." Genome Biology, 15.*
55. *Edgar, R. C. 2004. "MUSCLE: Multiple Sequence Alignment With High Accuracy and High Throughput." Nucleic Acids Res., 32: 1792–1797. doi: 10.1093/nar/gkh340*
56. *Kearse, M., Moir, R., Wilson, A., Stones-Havas, S., Cheung, M., Sturrock, S., et al. 2012. "Geneious Basic: An Integrated and Extendable Desktop Software Platform for the Organization and Analysis of Sequence Data." Bioinformatics, 28: 1647–1649. Doi: 10.1093/bioinformatics/bts199*
57. *Behrens, S., Fuchs, B. M., Mueller, F., and Amann, R. 2003. "Is the In Situ Accessibility of the 16S rRNA of Escherichia Coli for Cy3-Labeled Oligonucleotide Probes Predicted by a Three-Dimensional Structure Model of the 30S Ribosomal Subunit?" Appl. Environ. Microbiol., 69: 4935–4941. Doi: 10.1128/AEM.69.8.4935-4941.2003*
58. *Behrens, S., Rühland, C., Inácio, J., Huber, H., Fonseca, Á., Spencer-Martins, I., et al. 2003. "In Situ Acessibility of Small-Subunit rRNA of Members of the Domains Bacteria, Archea, and Eucarya to Cy3-Labeled Oligonucleotide Probes." Appl. Environ. Microbiol. 69, 1748–1758. doi: 10.1128/ AEM.69.3.1748–1758.2003*
59. *Kibbe, W. A. 2007. "OligoCalc: An Online Oligonucleotide Properties Calculator." Nucleic Acids Res., 35 : W43–W46. Doi: 10.1093/nar/gkm234*
60. *Altschul, S. F., Gish, W., Miller, W., Myers, E. W., and Lipman, D. J. 1990. "Basic Local Alignment Search Tool." J. Mol. Biol., 215: 403–410. Doi: 10.1016/S0022-2836(05)80360-2*
61. *Manz, W., Amann, R., Ludwig, W., Wagner, M., and Schleifer, K. H. 1992. "Phylogenetic Oligodeoxynucleotide Probes for the Major Subclasses of Proteobacteria - Problems and Solutions." Systematic Appl. Microbiol., 15: 593–600. Doi: 10.1016/S0723-2020(11)80121-9*
62. *Lin, X. J., Wakeham, S. G., Putnam, I. F., Astor, Y. M., Scranton, M. I., Chistoserdov, A. Y., et al. 2006. "Comparison of Vertical Distributions of Prokaryotic Assemblages in the Anoxic Cariaco Basin and Black Sea by Use of Fluorescence in Situ Hybridization." Appl. And Environ. Microbiol., 72: 2679–2690. Doi: 10.1128/aem.72.4.2679-2690.2006*
63. *Amann, R. I., Binder, B. J., Olson, R. J., Chisholm, S. W., Devereux, R., and Stahl, D. A. 1990. "Combination of 16s Ribosomal-Rna-Targeted Oligonucleotide Probes With Flow-Cytometry for Analyzing Mixed Microbial-Populations." Appl. Environ. Microbiol., 56: 1919–1925. Doi: 10.1128/aem.56.6.1919-1925.1990*
64. *Cambon-Bonavita, M.-A., Aubé, J., Cueff-Gauchard, V., Reveillaud, J. 2021. "Niche partitioning in the Rimicaris exoculata holobiont: the case of the first symbiotic Zetaproteobacteria." Microbiome, 9:87.*
65. *Zaplana, T., Miele, S., and Tolonen, A. C. 2024. "Lachnospiraceae are emerging industrial biocatalysts and biotherapeutics." Frontiers in Bioengineering and Biotechnology. Doi: 10.3389/fbioe.2023.1324396*
66. *Sorokin, D. Y., Tourova, T. P., Panteleeva, A. N., Kaparullina, E. N., and Muyzer, G. 2021. "Anaerobic utilization of pectinous substrates at extremely haloalkaline conditions by Natranaerovirga pectinivora gen. nov., sp. nov., and Natranaerovirga hydrolytica sp. nov., isolated from hypersaline soda lakes. Extremophiles, 16:307-315. Doi : 10.1007/s00792-012-0431-6*
67. *Mitchell, A. L., Scheremetjew, M., Denise, H., Potter, S., Tarkowska, A., Qureshi, M. et al. 2018. "EBI Metagenomics in 2017: enriching the analysis of microbial communities, from sequences reads to assemblies." Nucleic Acid Research, 4. Doi:*

10.1093/nar/gkx967

68. *Beresford-Jones, B. S., Forster, S. C., Stares, M. D., Notley, G., Viciani, E., Browne, H. P. et al. 2022. "The mouse gastrointestinal bacteria catalogue enables translation between the mouse and human gut microbiotas via functional mapping". Celle Host & Microbe, 30: 124-138. https://doi.org/10.1016/j.chom.2021.12.003.*
69. *Lesker, T. R., Durainaj, A. C., Gálvez, E. J. C., Lagkouvardos, I., Baines, J. F., Clavel, T. et al. 2020. "An integrated metagenome catalog reveals new insights into the murine gut microbiome." Cell Reports. Doi: 10.1016/j.celrep.2020.02.036*
70. *Winnen, B., Hvorup, R. N., & Saier Jr, M. H. 2003. "The tripartite tricarboxylate transporter (TTT) family." Research in Microbiology, 154(7): 457-465.*
71. *Ravaux, J., Zbinden, M., Voss-Foucart, M. F., Compère, P., Goffinet, G., and Gaill, F. 2003. 'Comparative degradation rates of chitinous exoskeletons from deep-sea environments." Mar Biol., 143:405–12.*
72. *Lobo, M. D. P., Silva, F. D. A., Landim, P. G. D. C., Da Cruz, P. R., De Brito, T. L., De Medeiros, S. C. et al. 2013. "Expression and efficient secretion of a functional chitinase from Chromobacterium violaceum in Escherichia coli." BMC biotechnology, 13: 1-15.*
73. *Xiao, X., Saito, A., Majka, J., Schlösser. 2002. "The novel Streptomyces olivaceoviridis ABC transporter Ngc mediates uptake of N-acetylglucosamine and N,N'-diacetylchitobiose." Mol. Genet. Genomics, 267 :429-239. Doi: 10.1007/s00438-002-0640-2*
74. *Walter, A., and Mayer, C. 2019. "Peptidoglycan structure, biosynthesis, and dynamics during bacterial growth". Extracellular Sugar – based biopolymers Matrices, 12:237-299*
75. *Amano, C., Willhelm, U., Koch, T., Reinthaler, T., Hansman, R.L., Sintes, E. et al. 2024-Preprint. "Anaplerotic processes are key contributors to dark carbon fixation in the ocean. http://dx.doi.org/10.21203/rs.3.rs-4996540/v1*
76. *Raeburn, S., Rabinowitz, J.C. 1971. "Pyruvate:Ferredoxin oxidoreductase: II. Characteristics of the forward and reverse reactions and properties of the enzyme. Archives of Biochemistry and Biophysics, 146(1):23-33. https://doi.org/10.1016/S0003-9861(71)80037-1*
77. *Nørager, S., Jensen, K. F., Björnberg, O., & Larsen, S. 2002." E. coli dihydroorotate dehydrogenase reveals structural and functional distinctions between different classes of dihydroorotate dehydrogenases. Structur." 10(9), 1211-1223.*
78. *Jacq-Bailly, A., Benvenuti, M., Payne, N., Kpebe, A., Felbek, C., Fourmond, V., et al. 2021. "Electrochemical characterization of a complex FeFe hydrogenase, the electron-bifurcating Hnd from Desulfovibrio fructosovorans." Frontiers in Chemistry, 8: 573305.*
79. *Kpebe, A., Benvenuti, M., Guendon, C., Rebai, A., Fernandez, V., Le Laz, S., et al. 2018." A new mechanistic model for an O2-protected electron-bifurcating hydrogenase, Hnd from Desulfovibrio fructosovoran." Biochimica et Biophysica Acta (BBA)-Bioenergetics, 1859(12): 1302-1312.*
80. *Michael, A. J. 2018. "Polyamine function in archaea and bacteria." Journal of Biological Chemistry. 293(48); 18693-18701.*
81. *Nakamura, A., Kurihara, S., Takahashi, D., Ohashi, W., Nakamura, Y., Kimura, S., et al. 2021. "Symbiotic polyamine metabolism regulates epithelial proliferation and macrophage differentiation in the colon." Nature communications, 12(1): 2105.*
82. *Li, L., Wang, M., Li, L., Du, Z., Sun, Y., Wang, X., et al. 2020. "Endosymbionts of metazoans dwelling in the PACManus hydrothermal vent: diversity and potential adaptive features revealed by genome analysis." Applied and Environmental Microbiology, 86(21); e00815-20.*
83. *Speare, L., Zhao, L., Pavelsky, M. N., Jackson, A., Smith, S., Tyai, B. et al. 2024 – Preprint. "Flagella are required to coordinately activate competition and host colonization factors in response to a mechanical signal." https://doi.org/10.1101/2023.12.31.573711*
84. *Haft, D. H., Selengut, J. Mongodin, E. F., Nelson, K. E. 2005. "A guild of 45 CRISPR-associates (Cas) protein families and multiple CRISPR/Cas subtypes exist in prokaryotic genomes." PLOS Computational Biology, 1 (6). Doi: 10.1371/journal.pcbi.0010060*
85. *Flores, G. E., J. H. Campbell, J. D. Kirshtein, et al. 2011. "Microbial Community Structure of Hydrothermal Deposits From Geochemically Different Vent Fields Along the Mid-Atlantic Ridge." Environmental Microbiology 13: 2158–2171.*

https://doi.org/10.1111/j.1462-2920.2011.02463.x.

86. *Hügler, M., A. G.rtner, and J. F. Imhoff. 2010. "Functional Genes as Markers for Sulfur Cycling and CO2 Fixation in Microbial Communities of Hydrothermal Vents of the Logatchev Field." FEMS Microbiology Ecology 73: 526–537. https://doi.org/10.1111/j.1574-6941.2010.00919.x.*
87. *Vogt, G. 2021. "Synthesis of diverse enzymes, food processing, and nutrient absorption in decapod crustaceans: a comparison to the mammalian model of digestion." Zoology, 147:125945.*
88. *Corbari, L., Zbinden, M., Cambon-Bonavita, M.-A., Gaill, F., Compère, P. 2008. "Bacterial symbionts and mineral deposits in the branchial chamber of the hydrothermal vent shrimp Rimicaris exoculata: relationship to moult cycle." Aquat Biol., 1:225–38*
89. *Capovilla, G., Castro, K. G., Collani, S., Kearney, S. M., Kehoe, D. M., and Chisholm, S. W. 2023. "Chitin degradation by Synechococcus WH7803." Scientific Reports, 13: 19944. https://doi.org/10.1038/s41598-023-47332-0*
90. *Hoell, I. A., Dalhus, B., Heggset, E. B., Aspmo, S. I., and Eijsink, C. G. 2006. "Crystal structure and enzymatic properties of a bacterial family 19 chitinase reveal differences from plant enzymes. The FEBS Journal.273:4889-4900.*
91. *Monge, E.C., Tuveng, T. R., Vaaje-Kolstad, G., Eijsink, V. G. H., and Gardner, J.G. 2018. "systems analysis of the glycoside hydrolase family 18 enzymes from Cellvibrio japonicus characterizes essential chitin degradation functions." Journal of Biological Chemistry. 293(10):3849-3859*
92. *Jan, C., J. M. Petersen, J. Werner, et al. 2014. "The Gill Chamber Epibiosis of Deep-Sea Shrimp Rimicaris exoculata: An In-Depth Metagenomic Investigation and Discovery of Zetaproteobacteria." Environmental Microbiology, 16: 2723–2738. https://doi.org/10.1111/1462-2920.12406*
93. *Thompson, C. L., Vier, R., Mikaelyan, A., Wienemann, T. and Brune, A. 2012. "'Candidatus Arthromitus' revised: segmented filamentous bacteria in arthropod guts are members of Lachnospiraceae." Environnemental Microbiology, 14(6): 1454-1465. Doi: 10.1111/J.1462-2920.2012.02731.x*
94. *Domadia, P., Swarup, S;, Bhunia, A;, Sivaraman, J. Dasgupta, D. 2007. "Inhibition of bacterial cell division protein FtsZ by cinnamaldehyde." Biochemical Pharmacology, 74(6): 831-840. https://doi.org/10.1016/j.bcp.2007.06.029*
95. *Bobere,k J. M., Stach, J., Good, L. 2020. "Genetic evidence for inhibition of bacterial division protein FtsZ by Berberine." PLoS One, 5:e13745 Public Library of Science.*
96. *Anderson, D. E., Kim, M. B., Moore, J. T., O'Brien, T. E., Sorto, N. A., Grove, C. I., et al. 2017. « Comparison of small molecule inhibitors of the bacterial cell division protein FtsZ and identification of a reliable cross-species inhibitor. » ACS Chem. Biol., 7:1918–28. American Chemical Society.*
97. *Catta-Preta, C. M. C., Brum, F. L., da Silva, C. C. Zuma, A. C., Elias, M. C., de Souza, W. et al. 2015. "Endosymbiosis in trypanosomatid protozoa: the bacterium division is controlled during the host cell cycle." Frontiers in Microbiology. doi: 10.3389/fmicb.2015.00520*
98. *Le Bloa, S., Boidin-Wichlacz, C., Cueff-Gauchard, V., Rosa, R. D., Cuvillier-Hot, V., Durand, L., et al. 2020. « Antimicrobial peptides and ectosymbiotic relationships: involvement of a novel type IIa crustin in the life cycle of a deep-sea vent shrimp. » Front. Immunol., 11:1511.*
99. *Hexun, Z., Miyake, T., Maekawa, T., Mori, H., Yasukawa, D., Ohno, M. and al. 2023. "High abundance of Lachnospiraceae in the human gut microbiome is related to high immunoscores in advanced colorectal cancer." Cancer Immunology, Immunotherapy, 72:315-326. https://doi.org/10.1007/s00262-022-03256-8*
100. *Zhang, X., Yu, D., Wu, D., Gao, X., Shao, F., Zhao, M., et al. 2023. "Tissue-resident Lachnospiraceae family bacteria protect against colorectal carcinogenesis by promoting tumor immune surveillance." Cell Host & Microbe, 31:418-432. https://doi.org/10.1016/j.chom.2023.01.013*
101. *Zaplana, T., Miele, S. and Tolonen, A. C. 2024. "Lachnospiraceae are emerging industrial biocatalysts and biotherapeutics." Frontiers in Bioengineering and Biotechnology. Doi : 10.3389/fbioe.2023.1324396*
102. *Tan, M. H., Park, H., Nobles, C. L., Karunadharma, P., Pan, L., Zhong, G. and al. 2021. "A more efficient CRISPR-Cas12a variant derived from Lachnospiraceae bacterium MA200." Molcular Therapy Nucleic Acids. https://doi.org/10.1016/j.omtn.2021.02.012.*

103. *Robertson, B. R., O'Rourke, J. L., Neilan, B. A., Vandamme, P., On, S. L.W., Fox, J. G., et al. 2005. « Mucispirillum schaedleri gen. Nov., sp. nov., a spiral-shaped bacterium colonizing the mucus layer of the gastrointestinal tract of laboratory rodents. » Int. J. Syst. Evol. Microbiol., 55, 1199–204. Microbiology Society.*

104. *Loy, A., Pfann, C., Steinberger, M., Hanson, B., Herp, S., Brugiroux, S., et al. 2017. « Lifestyle and horizontal gene transfer-mediated evolution of Mucispirillum schaedleri, a core member of the murine gut microbiota. » mSystems,2:e00171–16.*

105. *Herp, S., Brugiroux, S., Garzetti, D., Ring, D., Jochum, L. M., Beutler, M., et al. 2019. « Mucispirillum schaedleri antagonizes salmonella virulence to protect mice against colitis. » Cell Host Microbe, 25:681–694.e8.*

Figures

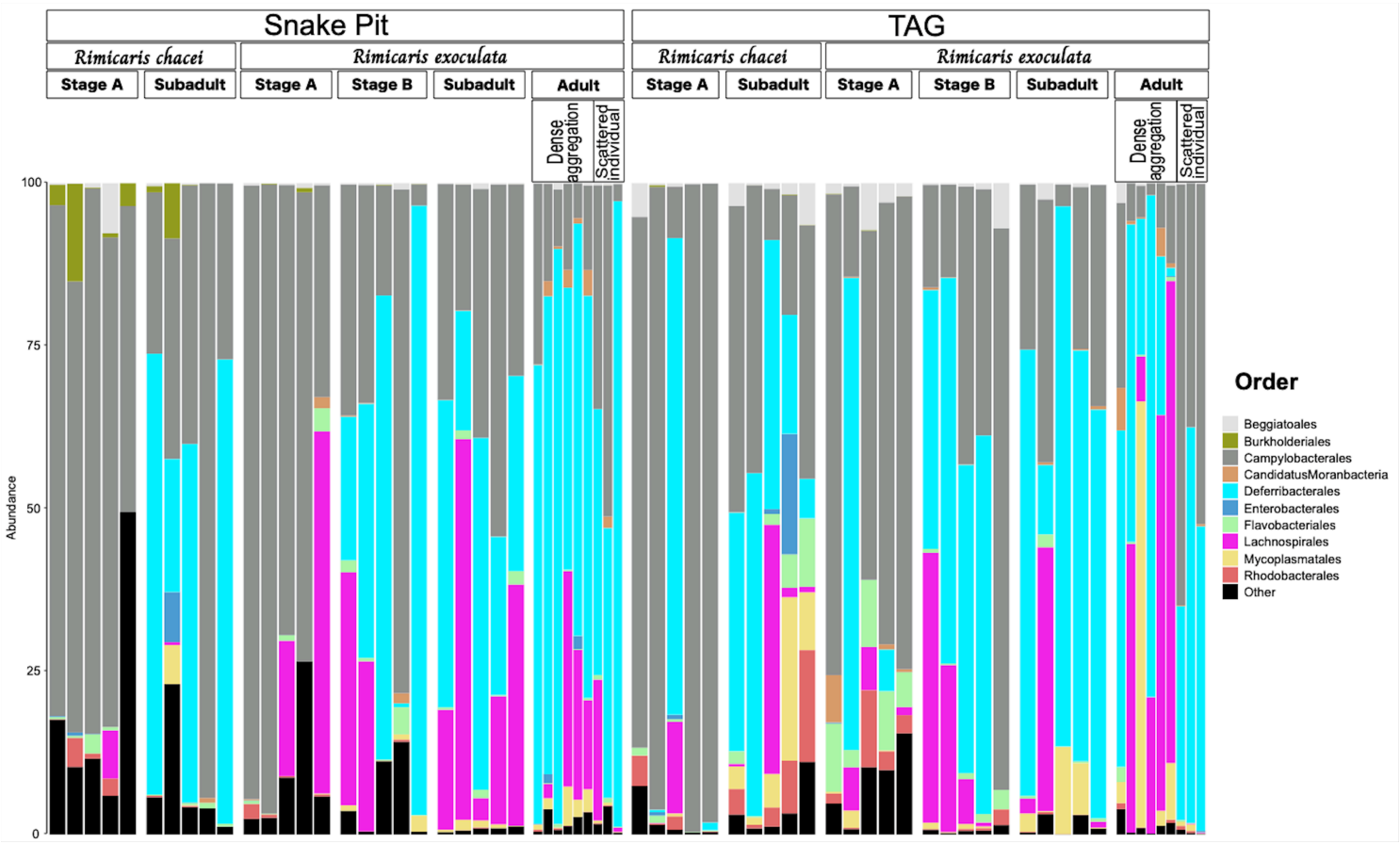


Figure 1

Bacterial composition at the order-level in the midgut tube samples of shrimp at different life stages, species and sites.

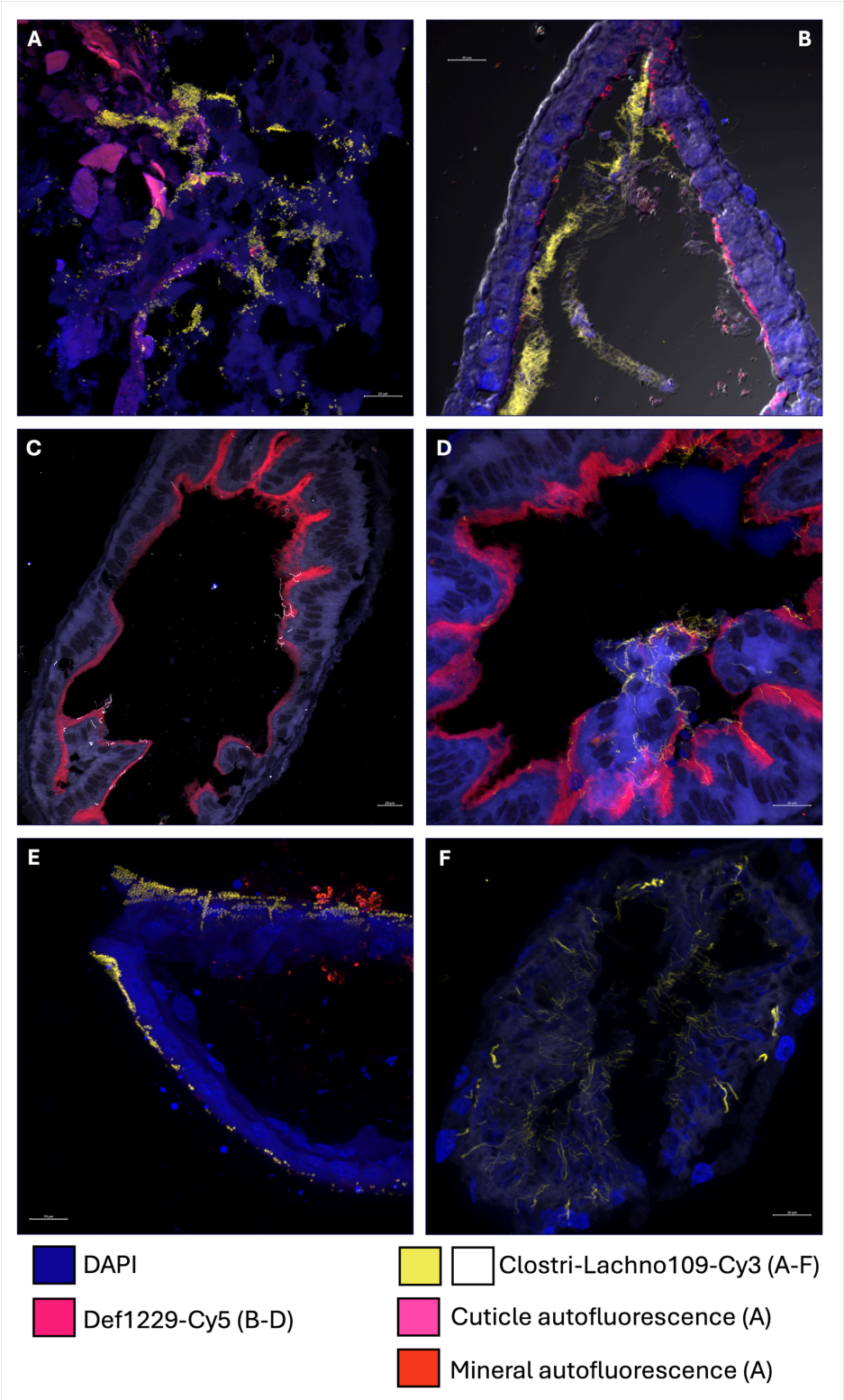


Figure 2

Observation of *Lachnospirales* and *Candidatus*Microvillispirillaceae in different midgut tube sections of *Rimicaris* specimens. *Lachnospirales*were hybridized with the specific probe Clostri-Lachno109-Cy3 (white in **C**, otherwise yellow) and *Ca.*Microvillispirillaceae were hybridized with the specific probe Def1229-Cy5 (red in **B-D**). Tissue cell nuclei are labeled with DAPI (blue). **(A)** Represents section through the midgut tube of *R. chacei* adult specimen. **(B-D)** Represent sections through the midgut tube of *R. exoculata* adult specimens. **(E-F)**Represent sections through the midgut tube of *R. exoculata* subadult specimens. All the pictures were taken with the Apotome® slider. DIC was used for **B**. Scale bar = 10 mm (**A-F**).

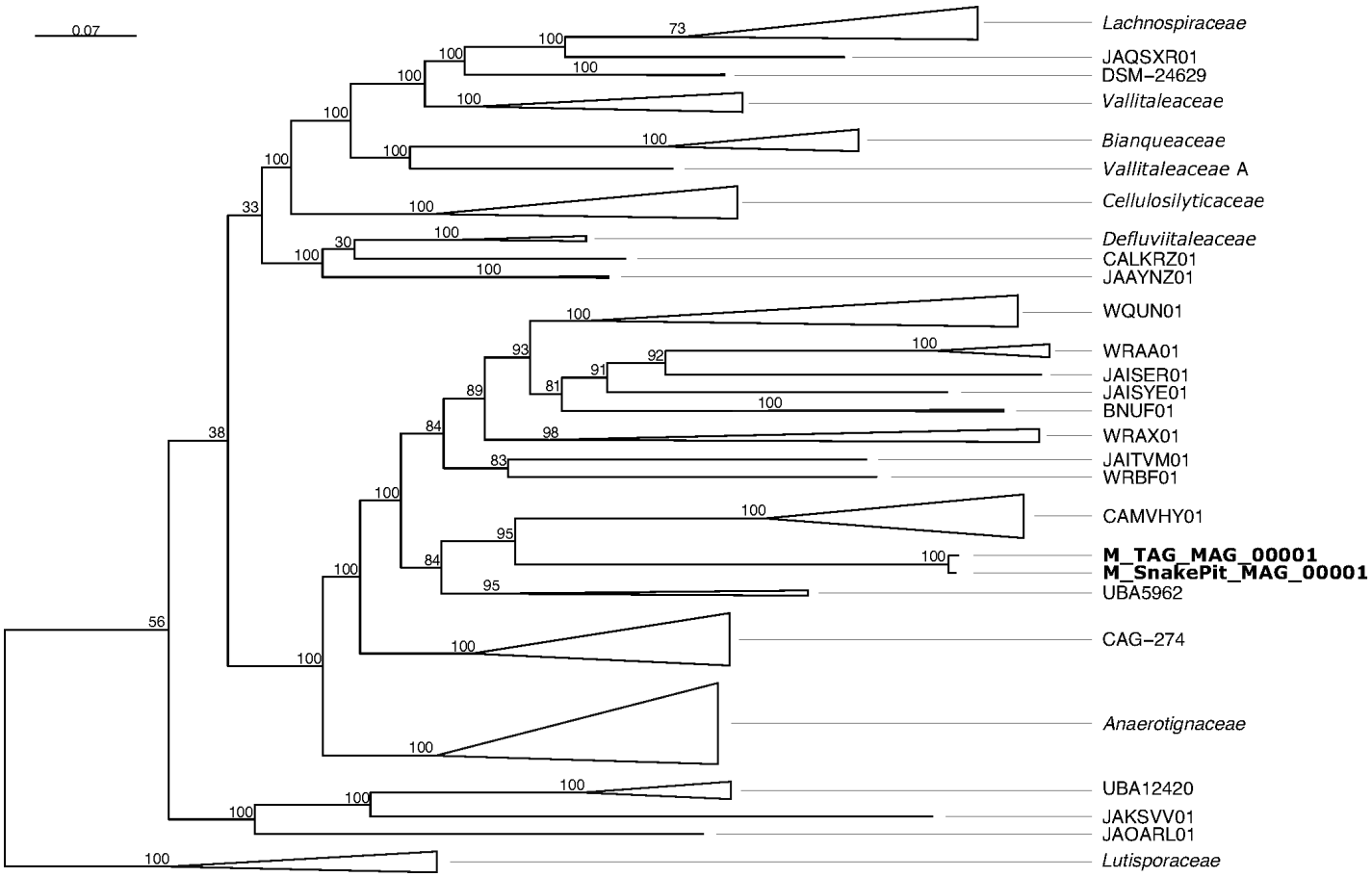


Figure 3

Maximum likelihood phylogenetic tree using IQ-TREE v2.0.3 with the “WAG” general matrix model and 1000 bootstrap replicates visualized using ggtreeExtra package for *Lachnospirales*.

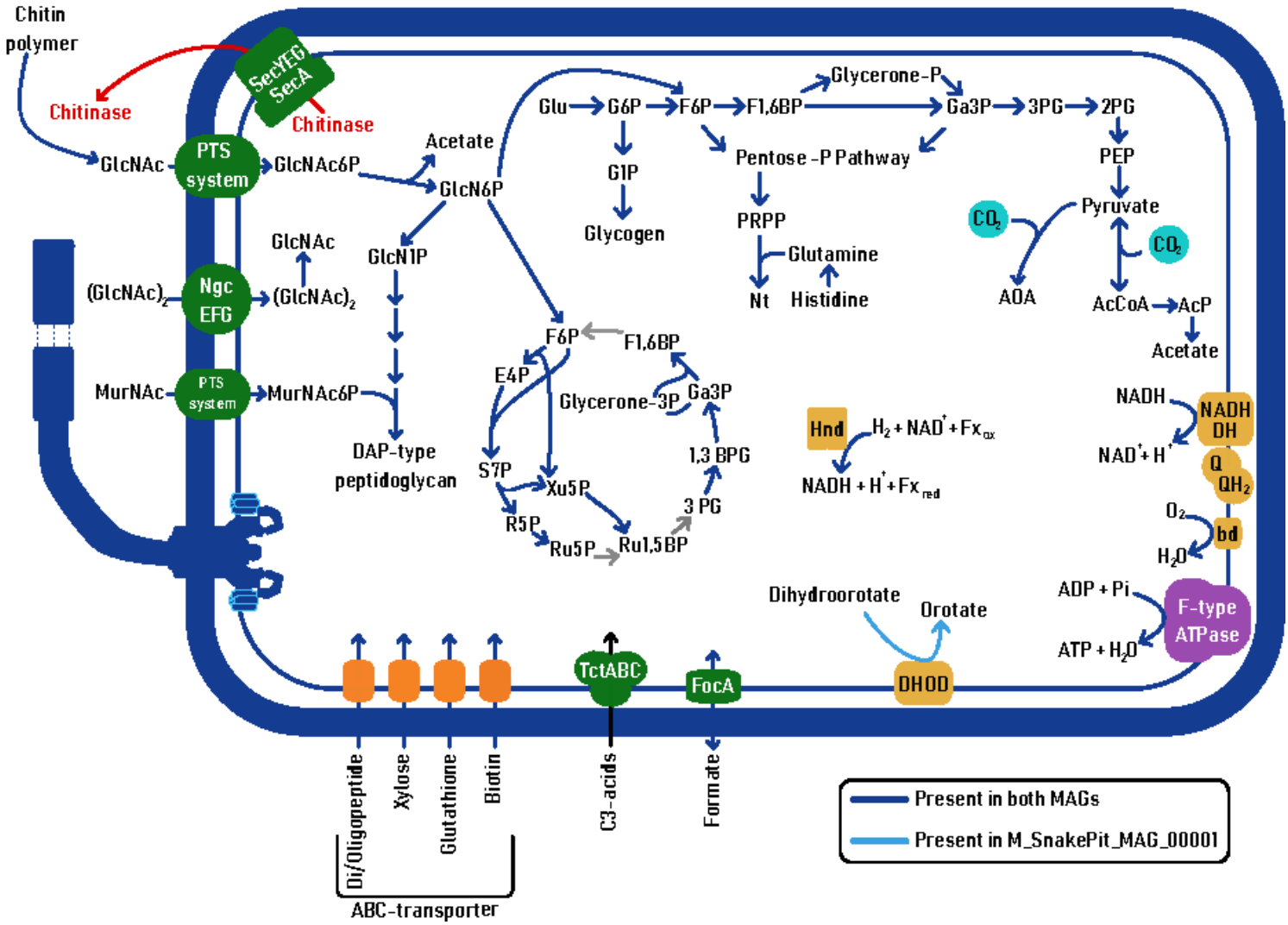


Figure 4

Schematic representation of the predicted metabolic potentials within the two *Lachnospirales*MAGs. In grey are represented the pathways not retrieved in the MAGs.

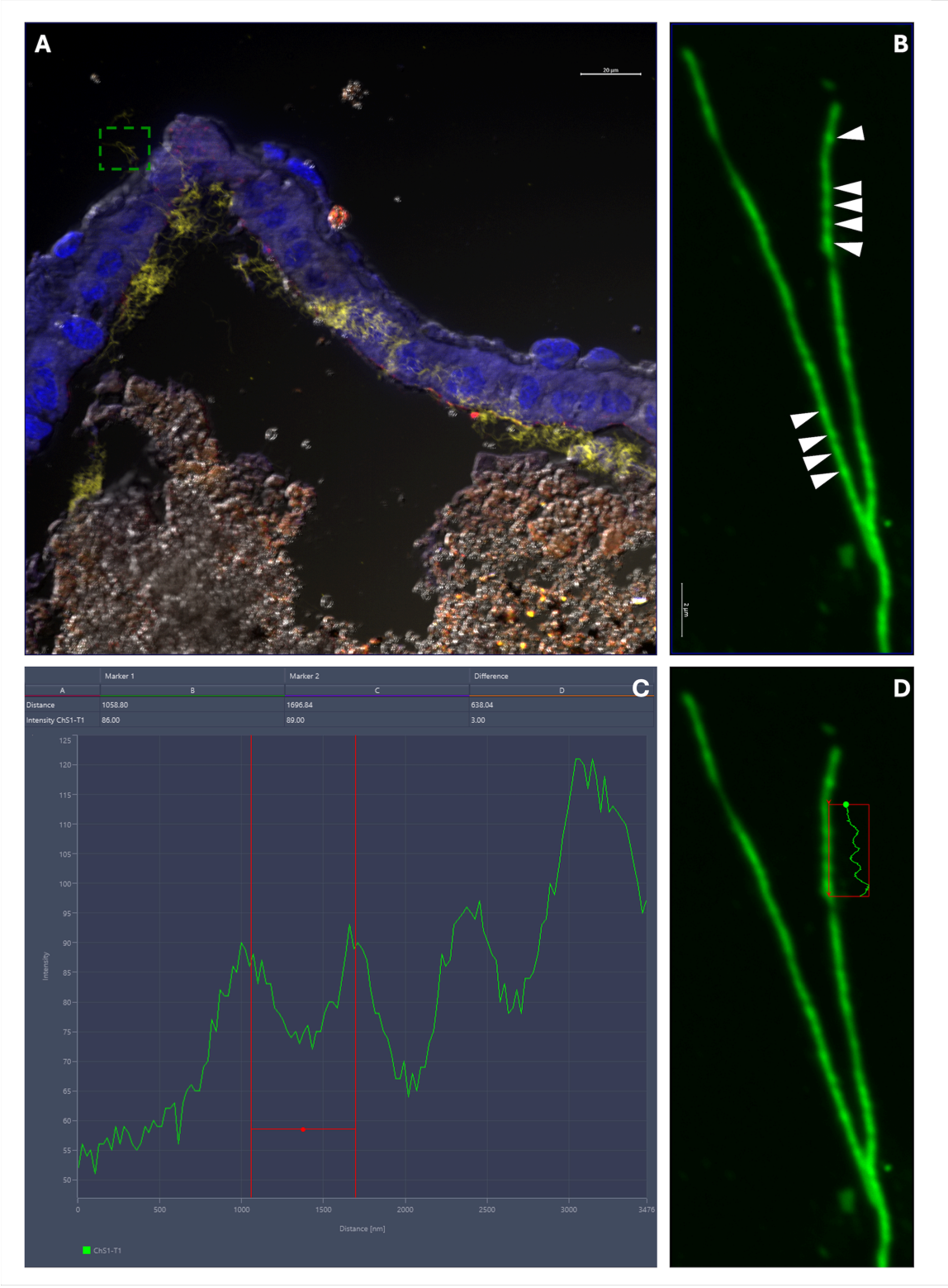


Figure 5

Chromosome observation of *Lachnospirales* using YOYO^{TM}-1dye labeling. **(A)** Represents section through the midgut tube of *R. exoculata* adult specimen (taken with Apotome and DIC). *Lachnospirales* were hybridized with the specific probe Clostri-Lachno109-Cy3 (yellow) and *Ca.*Microvillispirillaceae were hybridized with the specific probe Def1229-Cy5 (red). Tissue cell nuclei are labeled with DAPI (blue). The green square is image **B** and **D** with a closer view. Scale bar = 20 mm. **(B)** YOYO^{TM}-1dye labeling reveals several bacterial chromosomes per cell (green balls pointed by white arrows). Cells are non-segmented. Scale

bar = 2 mm. **(C)** represents the fluorescence intensity profile within the bacterial cell (**D**) highlighting that chromosomes are regularly spaced between 0.6 to 0.8 mm.

Supplementary Files

This is a list of supplementary files associated with this preprint. Click to download.

- Additionalfile1.docx
- Additionalfile2.xlsx
- Additionalfile3.docx
- LegendsAdditionalfile2.docx